CONSTRUCTION OF ONE-TENTH SCALE MODEL OF THE XFV-12A AND CANARD PERFORMANCE TEST

James Edward Killian

NAVAL POSTGRADUATE SCHOOL
Monterey, California

THESIS

CONSTRUCTION OF ONE-TENTH
SCALE MODEL OF THE XFV-12A
AND CANARD PERFORMANCE TEST

by

James Edward Killian
and
Adrian Tracy Doryland

Thesis Advisor: A. E. Fuhs

March 1974

Construction of One-Tenth Scale Model of the XFV-12A and Canard Performance Test

by

James Edward Killian
Lieutenant Commander, United States Navy
B.S., United States Naval Academy, 1963

and

Adrian Tracy Doryland
Lieutenant, United States Navy
B.S., University of Texas, 1966

Submitted in partial fulfillment of the requirements for the degree of

MASTER OF SCIENCE IN AERONAUTICAL ENGINEERING

from the

NAVAL POSTGRADUATE SCHOOL
March 1974

ABSTRACT

The XFV-12A is a high performance, VTOL, fighter/attack aircraft which incorporates ejectors in the wings and canards for thrust augmentation. During transition from VTOL to normal flight, the interaction between downflow of the lifting jets and relative flow from forward flight generates vortices distinct from airfoil circulation. These vortices are associated with the bending of the lifting jets resulting in induced velocities at the aircraft; the magnitude and influence of the vortices are unknown. The object of this thesis was to prepare a suitable one-tenth scale semi-span model of the XFV-12A for a smoke tunnel flow visualization study to explore vortex development. Performance testing was conducted on the canard augmentor, which resulted in a gross augmentation ratio of 1.34 and mass flow ratio of 6.84.

TABLE OF CONTENTS

LIST OF ILLUSTRATIONS

LIST OF SYMBOLS

Symbol	
A_1	Primary flow outlet area
A_2	Diffuser throat area
A_3	Diffuser outlet area
A_{1t}	Total A_1 for canard and wing
P	Static pressure
P_a	Ambient pressure
P_t	Pressure in air supply tanks
Re	Reynolds Number
T	Thrust
T_i	Isentropic thrust
T_1	Thrust derived from primary air flow
T_3	Thrust from mixed flow
V_1	Primary flow velocity
V_2	Velocity at diffuser throat
V_3	Diffuser outlet velocity
a	Radius of curvature
b	Coanda slot width
$\dot{m}_1$	Mass flow rate of primary air
$\dot{m}_3$	Mass flow rate of mixed air
t	Run time
ΔP	Pressure differential
θ_{sep}	Angle of flow separation for Coanda jet
ν	Kinematic viscosity

Symbol	
ρ	Density
Φ	Augmentation ratio
Φ_g	Gross augmentation ratio

ACKNOWLEDGMENT

The authors express their sincere appreciation to Professor Allen Fuhs of the Department of Aeronautics, Naval Postgraduate School, Monterey, California, for his assistance and guidance. Sincere appreciation is also extended to Mr. Ronald Ramaker and Mr. Gordon Gulbranson of the Department of Aeronautics for their effort in the construction of the model and to Assistant Professor Thomas M. Houlihan for use of compressed air facilities.

I. INTRODUCTION

A. BACKGROUND ON XFV-12A

The Navy needs a high performance, supersonic, V/STOL aircraft capable of a fighter/attack mission to operate from sea control ships in the 1980's. The Columbus Aircraft Division of North American Rockwell has been awarded a contract to develop the XFV-12A, a Mach two plus aircraft which utilizes ejector augmentation in the wings and canards to attain V/STOL. This aircraft is unique in its design and, if successful, could constitute a major aeronautical engineering achievement with substantial contributions to the future of both military and civilian aviation.

The XFV-12A has its wings installed aft and canards forward of the center of gravity. In the V/STOL regime of flight the tailpipe is plugged with a diverter and the engine exhaust is routed to ejectors in the aft sections of the wings and canards. The ejectors run spanwise; and due to the ejector principle as described in Section IIA, large quantities of outside air are drawn into the ejectors resulting in thrust augmentation. The overall effect is that the aircraft should be able to attain vertical flight with an installed engine thrust-to-weight ratio of less than one. If the required specifications are met, the most immediate advantage is that the engine may be sized for the mission vice the V/STOL flight regime. To attain sufficient

thrust augmentation, Coanda blowing (Section IIB) and hypermixing nozzles (Section IIC) are incorporated in the wing and canard ejectors.

B. THE VORTEX PROBLEM

Lift has been associated with bound vortices and trailing vortex sheets as far back in the literature as Betz, Prandtl, and Helmholtz. For a conventional wing a system of bound vortices is concentrated along the quarter chord line, and a trailing vortex sheet follows in accord with the variation of bound vorticity along the span.

The XFV-12A will conform to the theory in horizontal flight with the ejectors closed. In the V/STOL transition regime (as the wing is developing circulation with the ejectors open), an unexplored area of vortex development may occur. During transition from VTOL to normal flight, the interaction between downflow of the lifting jets and relative flow from forward flight generates vortices distinct from airfoil circulation. These vortices, which are associated with the bending of the lifting jets, are shed from the edges of the jets. The system of vortices induces velocities at the aircraft; the magnitude and influence of these velocities are unknown.

The object of this thesis was to prepare a suitable one-tenth scale semi-span model of the XFV-12A for a flow visualization study to explore vortex development. Also, components of the model were tested.

II. AUGMENTATION THEORY

A. EJECTOR PRINCIPLE

A basic ejector is comprised of a primary nozzle and a shroud as depicted in Figure 1. Consider high energy primary air expelled from the primary nozzle, causing mixing with the original air in the mixing duct due to shear stresses. The resulting flow through the confined area causes a reduction in the mean pressure which in turn results in entrainment of ambient air from outside the shroud. A momentum analysis would reveal that the flux of momentum across the exit plane contributes to the thrust produced by the entire system. The thrust augmentation ratio Φ is defined as follows:

$$\Phi = T/T_i$$

where T is the thrust produced by the nozzle-shroud system, and T_i is the thrust that would be produced by an isentropic expansion of the flow from the primary nozzle without the shroud in place. This ratio will be greater than one if the process is properly accomplished.

The Navy has specified that the augmentation ratio Φ for the XFV-12A must be equal to or greater than 1.55. After consultation with engineers from North American Rockwell, it was felt that the one-tenth scale model built

should have a Φ of at least 1.2 for flow visualization results to be considered valid.

B. COANDA EFFECT

In Ref. 4, Quinn's experiments with a two-dimensional ejector indicated the necessity for wall blowing for an ejector to perform as a good thrust augmentor. In the XFV-12A design, wall energization is accomplished by Coanda blowing along the span of the diffuser flaps, plus endplate blowing at the roots and tips.

Design for the Coanda blowing of the one-tenth scale model is as depicted in Figure 2. The Coanda slot is a fixed part of each diffuser flap and therefore rotates when each individual flap rotates. The diffuser flaps are circular at the inlets of the ejectors, and the required turning angle for the Coanda blowing is approximately 110 degrees in all cases. The results attained from the Coanda blowing are twofold: (1) inlet losses are reduced as the entrained air enters the ejector, and (2) a "blanket" of high energy primary air is created which helps prevent separation in the diffuser section.

In Ref. 3, Newman described the flow of a two-dimensional jet around a circular cylinder (Fig. 3). Figure 4 is a plot of θ_{sep} vs. Reynolds number from Newman's findings. θ_{sep} is the angle of flow separation in degrees around the cylinder, and

$$Re = \left[\frac{(P-P_\infty)ba}{\rho \nu^2} \right] 1/2$$

where

$P-P_\infty$ = the supply pressure relative to that of the surroundings

b = the width of the slot

a = the radius of the cylinder

ρ = the density of the fluid

ν = the kinematic viscosity of the fluid

Figure 4 indicates θ_{sep} varies linearly for $1 \times 10^{-4} \leq Re \leq 3 \times 10^{-4}$ and is roughly independent of Re for $Re \geq 4 \times 10^{-4}$. At low Re Newman states that

$$\theta_{sep} = f\left[\frac{b}{a}, Re\right]$$

and if separation is sufficiently far from the slot (i.e., greater than 20°)

$$\theta_{sep} = f[Re]$$

C. HYPERMIXING NOZZLES

In Ref. 5, Quinn's experiments demonstrate a direct relation between ejector performance and mixing of primary and entrained air. Complete mixing theoretically requires an infinitely long mixing duct. As this is not feasible, an alternative for aircraft design is the hypermixing nozzle which causes longitudinal vortices inside the ejector. In our model, as in the XFV-12A, discrete nozzles blowing

primary air into the shroud alternate in direction 20° either side of centerline along the length of each ejector (Fig. 5). In addition, an enlarged slot at both the inboard and outboard ends directs primary air on the end-plates. The combination of hypermixing nozzles and Coanda blowing results in efficient entrainment, accelerated mixing, and acceptable diffuser lengths for aircraft design.

III. MODEL FABRICATION

The primary reason the XFV-12A was so adaptable to this study was the fact that the construction blueprints for the 0.2 scale model built by North American Rockwell were available. Having ready access to these blueprints precluded a complete model design workup on the part of the authors. Simple application of a scale factor was all that was needed to produce a model of the proper size and geometry to conduct the study.

Sizing of the model was based on two factors. The primary restriction on maximum model size was the cross-sectional area of the test section of the wind tunnel chosen for the study. It has been found in previous tunnel studies of various types of models that there is some doubt in the validity of the data obtained when the test span is greater than one-third the tunnel test section width. Therefore, with a test section width of five feet, the maximum allowable test span was twenty inches. To build a model with a span restricted to twenty inches meant selection of a 1/20 scale model. However, fabrication of parts of the augmentation system smaller than 1/10 scale would have been extremely difficult. Therefore the decision was made to build a 1/10 scale semi-span model.

Once a model size had been selected, the choice of fabrication materials was made with consideration given to weight, structural strength, cost, and ease of fabrication.

The initial decision was to construct the model entirely from wood but was ruled out because of the weight involved and the necessity of hollowing out a large portion of the fuselage for installation of the air augmentation system. It was also decided to construct the model in several distinct parts which would then have to be integrated into a whole model assembly.

The first piece to be constructed was the aircraft fuselage. With consideration for the factors mentioned before, the material selected for fuselage construction was fiberglass. The fuselage was made in the form of a fiberglass shell. The first step in the fuselage construction was the molding of a clay model of the port side of the aircraft fuselage as shown in Fig. 6. From this male model a female plaster mold was cast. Then the actual fuselage was made by laying up a fiberglass shell in the plaster mold to a thickness of about one-eighth inch. The wing and canard anhedral angles were built in at the root as an integral part of the fuselage shell. The finished fuselage with wing and canard attached is shown in Fig. 7.

The second piece fabricated was the vertical tail assembly. This was constructed from epoxy. The decision was made to use epoxy instead of fiberglass for ease of fabrication although this increased the weight of the tail assembly substantially. The finished vertical tail assembly is shown in Fig. 8.

The fixed forward portion of the wing was made of wood. It was attached to the fuselage by three threaded bolts which were imbedded in the wing beam. Naturally the fuselage shell had to be reinforced at all points of attachment. The vertical tail assembly was attached to the wing beam assembly with screws.

The fixed beam portion of the canard assembly was made from aluminum bar stock instead of wood. This choice was made because attachment to the fuselage was a difficult matter due to the proximity of the beam root to the opening of the engine inlet and diffuser in the forward part of the fuselage. The fixed canard beam was also the main structural support of the canard end plate in which the thrust augmenting ejector flap pivots were located.

The most difficult parts of the model to fabricate were the thrust augmenting ejector flaps. For both the wing and canard the fore and aft flaps have a Coanda slot formed into the leading edge contour, and the center ejectors required hypermixing nozzles machined into the leading edge. These nozzles were machined at an angle of 20° to the vertical with alternating direction for every other nozzle. For the canard the fore and aft flaps were made from wood with an aluminum plate screwed on to the leading edge to form the Coanda slots. Construction of the wing fore and aft flaps was accomplished in the same manner as for the canard, but all parts were made from aluminum. The reason for the change of materials was that it was felt that the aluminum structure would be

stronger and less likely to separate and deform when air pressure was applied to the augmentation system. Both center ejector flaps were made from aluminum bar stock and sheet metal. The hypermixing nozzles were machined from aluminum bar stock, and the airfoils were then formed from sheet metal and epoxied to the nozzle bar. Details of thrust augmenting ejector flaps can be seen in Figs. 9 and 10.

The final parts to be constructed were the canard and wing end plates in which the outboard pivots for the thrust augmenting ejector flaps were located. The pivot line for the fore and aft flaps of both the wing and the canard coincided with the air supply pipe centerline. However, the pivots for the center ejectors were vertically offset above the flaps. The offset pivot was required to ensure that the center ejector was centered between the two Coanda flaps at all angles of ejector operation.

IV. SMOKE TUNNEL

A. PHYSICAL DESCRIPTION

The Naval Postgraduate School smoke tunnel is located in the basement of Halligan Hall. It is a suck down facility powered by a 0.5 horsepower motor. The Jay Series 1000 variable pitch axivane fan gives the tunnel a speed capability of approximately zero to fifty ft./sec.

Smoke is injected through a tube which runs through the three-inch thick honeycomb that covers the entrance bell-mouth. The purpose of the honeycomb is to reduce turbulence of the in-drawn air and thus help to ensure that the stream-lines are straight when they reach the test section.

The test section is five feet by five feet. It is fully lighted, and there is a view window in one side of the tunnel. Cameras may be placed inside the tunnel downstream from the test section to take desired photographs of tests which are conducted.

B. WIND TUNNEL CORRECTION THEORY FOR V/STOL AIRCRAFT

The classical theory normally utilized for wind tunnel corrections for CTOL aircraft models is not accurate for V/STOL aircraft for two basic reasons. First, the representation of the wake, which is normally assumed to pass directly downstream in CTOL corrections, is entirely inadequate for V/STOL models where the wake may be deflected downward by as much as 90°. Second, since the entire lifting system

deflects air against the walls of the wind tunnel, the entire system for generating lift must be considered instead of only the "circulation" lift on which the corrections of CTOL theory are based. Thus it is seen that the fundamental requirement in developing a correction theory for V/STOL wind-tunnel tests is to treat a wake which may be deflected substantially downward from the horizontal [Ref. 1].

In ideal aerodynamic theory, flow over a circular cylinder of infinite length has been modeled by the superposition of a uniform stream upon a string of doublets along a line normal to the flow [Ref. 2]. Assuming the model is small in comparison to the wind tunnel, it is reasonable to assume that the wake of the lift system consists of a uniform distribution of point doublets along straight lines which begin at the model and extend to infinity. Since one is concerned with a flow which is deflected downward, the wake intersects the wind tunnel floor at some point below and behind the model. Beyond this point the wake flows along the floor. Again due to the downward deflection of the wake, one must consider both a wake of vertical doublets and a wake of horizontal doublets. Both wakes are colocated. In order to maintain zero flow through the floor, it is necessary to assume the existence of a mirror-image wake directly below the floor. The vertical doublets of the real and image wakes along the floor will merely cancel each other. When the doublets are longitudinal, the wake and its image along the floor add rather than subtract.

These wake and image systems are shown in Fig. 11 for a closed wind-tunnel floor (adapted from Ref. 1, Fig. 2).

To extend this theory to a model of finite size, consider the wake originating from the model as broken into segments, each representing the wake of only a portion of the model. The effect of each partial wake, as well as the interference of all the other partial wakes, in the wind-tunnel can then be added at each point on the model in order to obtain an overall correction. To be applicable to a thrust augmentation model like the XFV-12A, one must next consider a lifting system of two individual, equally loaded elements arranged one behind the other. Each element will then experience interference at its location due to itself and additional interference due to the presence of the other element. If the lifts of the two elements are assumed to vary according to the operating conditions, as they will for the XFV-12A wing and canard, it is not permissible to add together the effects of the lifting system on itself and the effect due to the presence of the other system. This is due to the fact that the systems have different lifts, drags, and momentum areas. Thus it is necessary to maintain the identity of the source of interference by finding four sets of interference factors. These are as follows: The interference at the front element due to its own presence, the interference at the rear element due to the presence of the front element, the interference at the

rear element due to its own presence, and the interference at the front element due to the presence of the rear element. One further step in modeling the flow system of the XFV-12A is realized by assuming the wake to be a sheet of doublets of finite size as outlined by utilizing the double layer distribution theory [Ref. 6]. This model would appear as in Fig. 12.

When this theory is actually applied to an experimental wind-tunnel model, it would be expected that the degree to which the wake is deflected downward would have a primary effect on the magnitude of the interference. For severe downward deflections, the corrections would be primarily determined by the floor of the tunnel and may be considered as identical to ground effect. Since ground effect is a function of the height above the floor, the vertical placement of the model in the wind-tunnel becomes important.

V. MODEL DESIGN

A. SIZING OF COANDA SLOTS AND HYPERMIXING NOZZLES

The performance of an ejector is highly dependent upon area ratios. The area ratios to be considered are first, A_3/A_1, the ratio of diffuser outlet area to the inlet area through which the primary air flows and second, A_3/A_2, the ratio of diffuser outlet area to the diffuser throat area.

Because North American Rockwell has the benefit of experience concerning the area ratios, A_3/A_1 and A_3/A_2, they were consulted to determine the best physical dimensions for the nozzles and Coanda slots utilized in the model. All augmentor flaps were both tapered and swept. Therefore to achieve the best mixing results it was felt that the Coanda slots and mixing nozzles should also have a tapered width.

For the canard, the forward Coanda slot was tapered from a width of 0.035 in. at the root to 0.015 in. at the tip. The aft Coanda slot was tapered from 0.040 in. at the root to 0.015 in. at the tip. The center ejector nozzle width tapered from 0.080 in. at the root to 0.030 in. at the tip. Although tapered width Coanda slots and nozzles were more desirable, the wing flaps were designed with a constant width along the flap length for both nozzles and Coanda slots. This was done for two reasons. The

calculated tip width values were in the range of 0.005 in. to 0.007 in. This presented some difficulty in machining and fitting tolerances. Secondly, and probably most important, it was felt that a very small area at the tip would possibly cause some flow restriction. Due to the fact that there is some inherent degradation in the flow as the distance from the flow source increases, this would have been very undesirable. Therefore the forward wing flap was constructed with a constant Coanda slot width of 0.017 in. The aft Coanda slot width was 0.018 in. The center ejector nozzle width was 0.035 in.

Sample calculations for comparison of the model's Coanda slot sizings with Newman's theory (presented in Section IB. are in Appendix A. As the Reynolds number varies with both the slot width and the radius of the required turning angle, a spanwise variation in Re resulted with the larger values at the roots. An average value of Re was calculated for each Coanda slot using a $P - P_\infty$ equal to 3 in. Hg (1.47 psi). Figure 4 was entered with these values of Re to find the theoretical value for θ_{sep}. The average Reynolds numbers varied from 1.015×10^4 for the aft wing Coanda slot to 1.404×10^4 for the aft canard Coanda slot. In all cases the average theoretical θ_{sep} was 150° or greater, which exceeds the required 110° and, therefore, is satisfactory.

B. OPERATING CONDITIONS

To obtain accurate quantitative data from a model study there must be dynamic similitude between model and prototype. This similitude requires that there be geometric similitude and kinematic similitude, i.e. the streamlines must be geometrically similar. Geometric similitude must be very exact, even to the projection of surface roughness. For strict dynamic similitude the Mach and Reynolds numbers must be the same for both model and prototype. This is generally impossible to achieve except on a full scale model [Ref. 7]. Since full scale testing is usually impractical as well as expensive, sacrifice in some area of similitude is expected.

Because of the limited speed of the NPS smoke tunnel (i.e. V_{max} = 50 ft/sec), it would be impossible to achieve Reynolds number similarity. To achieve Reynolds number similarity the tunnel would have to be capable of speeds ten times that of the actual aircraft or have density ten times atmospheric density. Velocities ten times actual values would be impractical because near-transonic or possibly supersonic speeds would be encountered and compressibility effects would also be a relevant factor. For the real aircraft in the VTOL or transition regime, one would certainly not expect to encounter transonic or supersonic velocities. The Mach number is not very relevant here because of the low subsonic flight regime in which the test was conducted.

However, one can scale the velocities. If the ejector velocities on the model are set at approximately 0.5 that of the operating aircraft, the tunnel can be run at 0.5 V_∞. Kinematic similarity is achieved.

VI. AIR SUPPLY AND PLUMBING

The existing compressed air supply for the smoke tunnel consists of two compressors rated at 17.2 ft^3/min and 49.5 ft^3min respectively at 125 pounds/in^2, and two 80 gallon tanks. The total mass flow rate of the compressors is 0.0843 lbm/sec.

The exit area from the model augmentors (including primary blowing and Coanda blowing for both the canard and wing) is 1.615 in^2. Assuming steady, incompressible flow and standard density at the nozzles and Coanda slots, a plot of $\dot{m}_1$ versus V_1 (Fig. 13) was made using the continuity equation:

$$\dot{m}_1 = \rho A_1 V_1$$

Velocities for V_1 for smoke tunnel testing are expected to vary in the range of 200 to 600 ft/sec. From Fig. 13 it can be seen that $\dot{m}_1$ should vary correspondingly from about 0.17 lbm/sec to 0.51 lbm/sec. Thus, it was deduced that the existing air supply is inadequate; and, therefore, three 400 gallon ASME coded tanks were purchased and will be installed in parallel with the two 80 gallon tanks. Total storage capacity will then be 1360 gallons, or 181.8 ft^3. Planned tank operating pressure is 125 lb/ft^2, and an estimate of run time with the system operating in

a blowdown capacity was made from:

$$t \simeq \frac{\text{(Volume of Tanks)}}{V_1 A_1} \left(\frac{P_t}{P_\infty}\right)$$

From Fig. 14 (a plot of t vs. V_1) it can be seen that run times vary from approximately 11 minutes to 3.7 minutes for V_1 equal to 200 ft/sec and 600 ft/sec respectively.

A two-inch pipe will run from the tanks through a shut-off valve and a regulator. A section of two-inch inner diameter hose will connect the outlet of the regulator to a plenum chamber (Fig. 15). The plenum has eight outlets for supplying air to the model via flexible tubing and may be metered with individual valves. The tubing will run from the plenum (situated outside the smoke tunnel) through the tunnel wall to the model which will be mounted on a splitter plate about six inches from the wall. Six of the outlets will be used to supply air to the two center ejectors and four Coanda slots. The additional two outlets may be used to create flow into the aircraft air intake by means of ejectors for more realistic tunnel testing. Mercury manometers will be connected to the entrance of each center ejector and diffuser flap for accurate pressure control and measurement.

VII. CANARD AUGMENTOR TEST

A. DESCRIPTION OF APPARATUS

As the air supply described in Section VI had not yet been constructed, a different supply was used for preliminary testing of the canard ejector performance. The system consisted of two 117 cubic feet tanks connected in parallel. A two-inch pipe led from the tanks through a shutoff valve and a regulator. A section of two-inch inner diameter hose was used to connect the outlet of the regulator to the inlet of the plenum chamber. See Fig. 15. The plenum was constructed from a forty-two inch section of six-inch steel pipe, and eight 5/8-inch inner diameter outlets were welded to the top with individual valves installed for metering the flow. A pressure gauge was installed for reading plenum pressure.

The canard ejector was mounted on a stand so that the center ejector and diffuser flaps could be fixed at various representative positions (Fig. 16). Tubes with 5/8-inch inner diameter were braised to the roots of the diffuser flaps, and a 3/4-inch inner diameter tube was braised to the root of the center ejector. These tubes protruded through the back of the stand and were connected to three outlets of the plenum with flexible hoses. Three mercury manometers were connected up to the entrance of the tubes in order to measure the air pressure entering the center

ejector and diffuser flaps for primary blowing and Coanda blowing respectively (Fig. 17). The other five outlets of the plenum were closed during canard testing.

A pressure rake was hooked up to a water manometer board and placed underneath the augmentor. The purpose of the rake was to measure chordwise pressure distributions at various positions along the span of the ejector. A special stand was constructed for the rake so that it would be a constant distance from the bottom of the augmentor when at different spanwise positions (Fig. 18).

B. EXPERIMENTAL PROCEDURE

The initial step in conducting a test run to obtain a pressure survey across the diffuser outlet was to stabilize the pressure at which the plenums in the diffuser flaps were set. This was done by regulating the pressure from the system plenum with the mercury manometers. The static pressure set with the manometers was three inches of Mercury. By utilization of the relation $V_1^2 = 2\Delta P/\rho$ and assuming incompressible flow, the velocity of the primary air from the Coanda slots and nozzles was calculated as 425.8 ft/sec. The ejector was set in the 90° position to simulate the VTOL configuration.

To determine the velocity at the diffuser outlet, the outlet area was divided into four sections. This permitted the integration of the velocity over the area by utilizing a summation technique. The pressure rake was placed across

the center of each of these four sections to obtain the survey as indicated in Fig. 19. The individual pressures sensed by the tubes of the pressure rake were displayed on the multiple water manometer board. For each pressure reading, V_3 was calculated from the relation $V_3^2 = 2\Delta P/\rho$. A set of sample calculations is included in Appendix B. As it was necessary to obtain a mean velocity for a given section, the velocities were summed over all readings taken for one survey and divided by the number of readings. A mean velocity for the entire diffuser outlet was then calculated by weighting each mean section velocity with the percentage of total area that the section area included and summing over the four sections. The mean velocity at the diffuser outlet was 83.38 ft/sec. Once the mean velocity at the diffuser exit had been determined, the mean mass flow rate at the diffuser outlet was calculated from the equation $\dot{m}_3 = \rho \bar{V}_3 A_3$. The mass flow rate due to the primary air flow through the center nozzles and Coanda slots had previously been calculated from the relation $\dot{m}_1 = \rho V_1 A_1$. Now that the velocities and mass flow rates of the primary air and the mixed flow had been determined, the gross thrust of each component was determined by $T_1 = \dot{m}_1 V_1$ and $T_3 = \dot{m}_3 V_3$. The gross diffuser augmentation ratio Φ_g was then determined as the ratio T_3/T_1.

VIII. EXPERIMENTAL RESULTS AND INTERPRETATION

The calculated gross value for augmentation ratio of the canard augmentor was 1.34. By use of tufts while blowing, it was visually apparent that the Coanda effect was consistent with the theory and the flow remained attached to the walls of the diffuser flaps over most of the augmentor (Fig. 20). Separation did occur in the vicinity of the roots and tips.

The ratio of mass rate of flow from the augmentor to that of the primary air was 6.84.

The pressure profiles for the four sections described in Section VIIB are plotted in Figure 21. These plots show that mixing decreased in the center of the ejector as the pressure rake was moved outboard. Average velocity for sections one through three were relatively close, varying from 99.06 ft/sec for section one to 100.18 ft/sec for section two. Average velocity for section four, however, was 55.24 ft/sec. This significant velocity drop may warrant additional end wall blowing at the root.

IX. CONCLUSIONS AND RECOMMENDATIONS

A. CONCLUSIONS

The results obtained indicate that the augmentor did function satisfactorily. The Coanda flow remained attached to the flaps except near the end walls where separation was experienced. Separation was due to a lack of sufficient end wall blowing and the fact that the augmentor box was not tightly closed. The entrainment of secondary air did occur as outlined in the ejector principle in Section II.

Although the hypermixing nozzles did promote good mixing, the pressure distributions show that mixing efficiency apparently decreased near the tip region. Perhaps a solution to this would be to vary the nozzle angle from 20° at the root to some smaller angle at the tip. This would eliminate the region of low pressure directly under the nozzles which is due to the fact that the primary air in this region is all blown outward and there is no mixing in the center.

B. RECOMMENDATIONS

For future studies with this model, some system must be designed to enhance blowing along the end walls. This would prevent separation of the Coanda flow near the end walls and also promote much more efficient mixing in this region. One such system might include nozzles fixed along the side of the fuselage to ensure that a continuous blanket

of air is blown along the end wall. The wing center ejector has not been fabricated, but a recommendation has been made to vary the nozzle outlet angle from 20° at the root to some smaller angle at the tip to promote more efficient mixing in the center of the augmentor. It is also recommended that some system be devised to ensure that the augmentor box is tightly closed. This would prevent the mixed air from escaping the diffuser at some point other than the intended outlet.

One area of concern with regard to the canard flaps was that they might not withstand pressures higher than those to which they were subjected in these tests. The reason for this concern is because of the wood construction. Therefore it is recommeded that the canard flaps be refabricated from aluminum, as are the wing flaps, before further tests are conducted.

One final recommendation is made to permit utilization of the engine inlet diffuser. A system should be devised to permit boundary layer blowing along the diffuser inlet plate. With a wind-tunnel velocity this blowing would help entrain air through the engine inlet. The total effect of simulation of the engine inlet flow in addition to the wing-canard thrust augmentation system would present a very realistic representation of the operation of the actual aircraft.

APPENDIX A

COANDA COMPARISON CALCULATION

Sample calculations for canard forward diffuser flap Coanda slot:

$$Re = \left[\frac{\Delta P b a}{\rho \nu^2}\right]^{1/2}$$

ΔP = 3 in. Hg. = 1.4736 psi

ρ = 0.00238 slugs/ft^3

$\nu = 1.8 \times 10^{-4}$ ft^2/sec

Root: a = 0.375 in

b = 0.035 in

Re = 1.584×10^4

Tip: a = 0.09375 in

b = 0.015 in

Re = 0.519×10^4

Average Re = 1.052×10^4

From Fig. 4, $\theta_{sep} \cong 150°$

APPENDIX B

DIFFUSER OUTLET VELOCITY CALCULATIONS

ΔP actual = $\Delta P \sin 30°$

$$V_3^2 = \frac{2\Delta P}{\rho}$$

For $\Delta P = 2.25$ in H_2O

$$V_3 = 100.03 \text{ ft/sec}$$

V_3 average for entire diffuser is 83.38 ft/sec

$$\dot{m}_1 = \rho V_1 A_1 = 0.1936 \text{ lbm/sec}$$

$$\dot{m}_3 = \rho V_3 A_3 = 1.325 \text{ lbm/sec}$$

$$T_1 = \dot{m}_1 V_1 = 82.435 \text{ lbm ft/sec}^2$$

$$T_3 = \dot{m}_3 V_3 = 110.45 \text{ lbm ft/sec}^2$$

$$\Phi_g = \frac{T_3}{T_1} = 1.34 = \text{Gross Augmentation Ratio}$$

$$\frac{\dot{m}_3}{\dot{m}_1} = 6.84 = \text{Mass Flow Ratio}$$

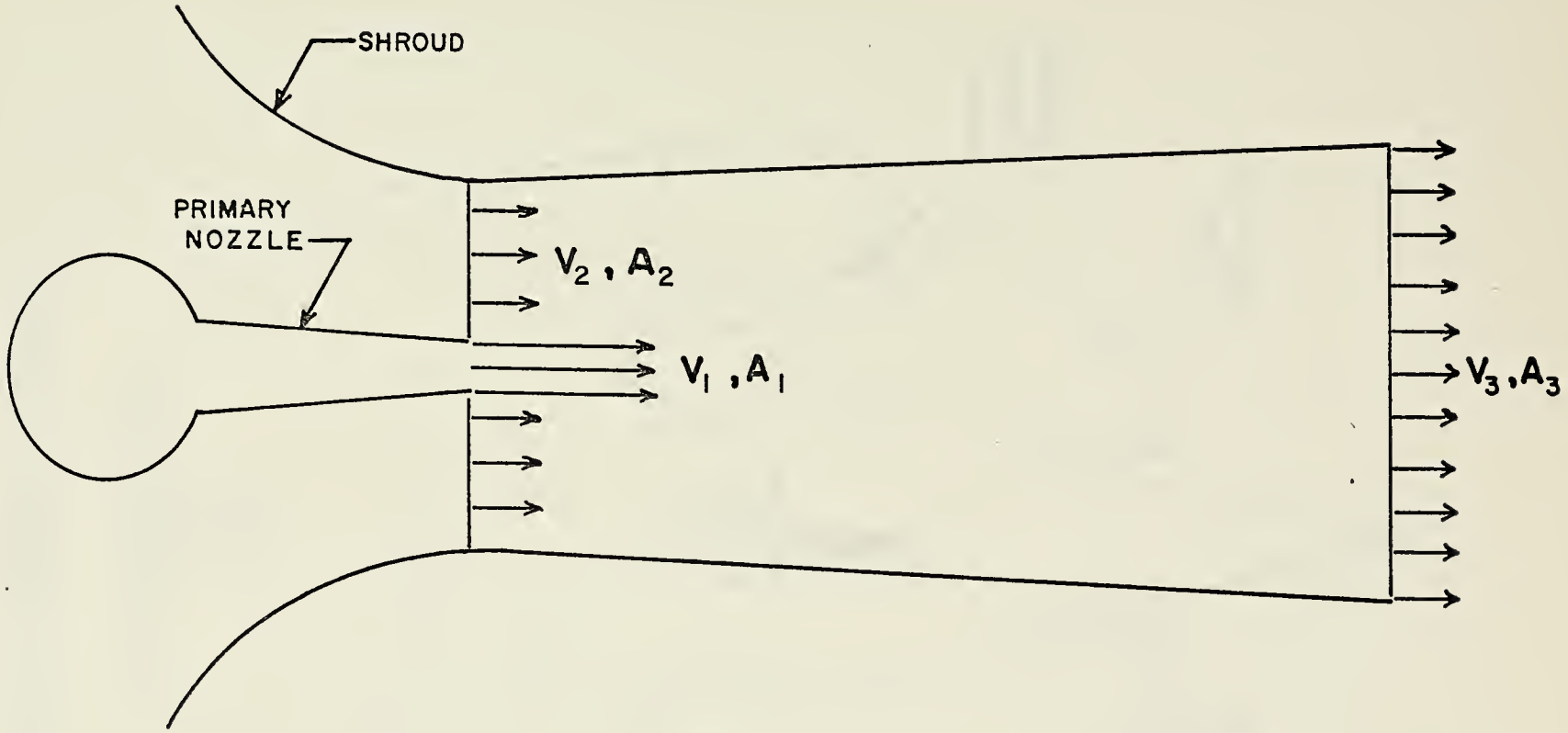

FIGURE I. BASIC EJECTOR

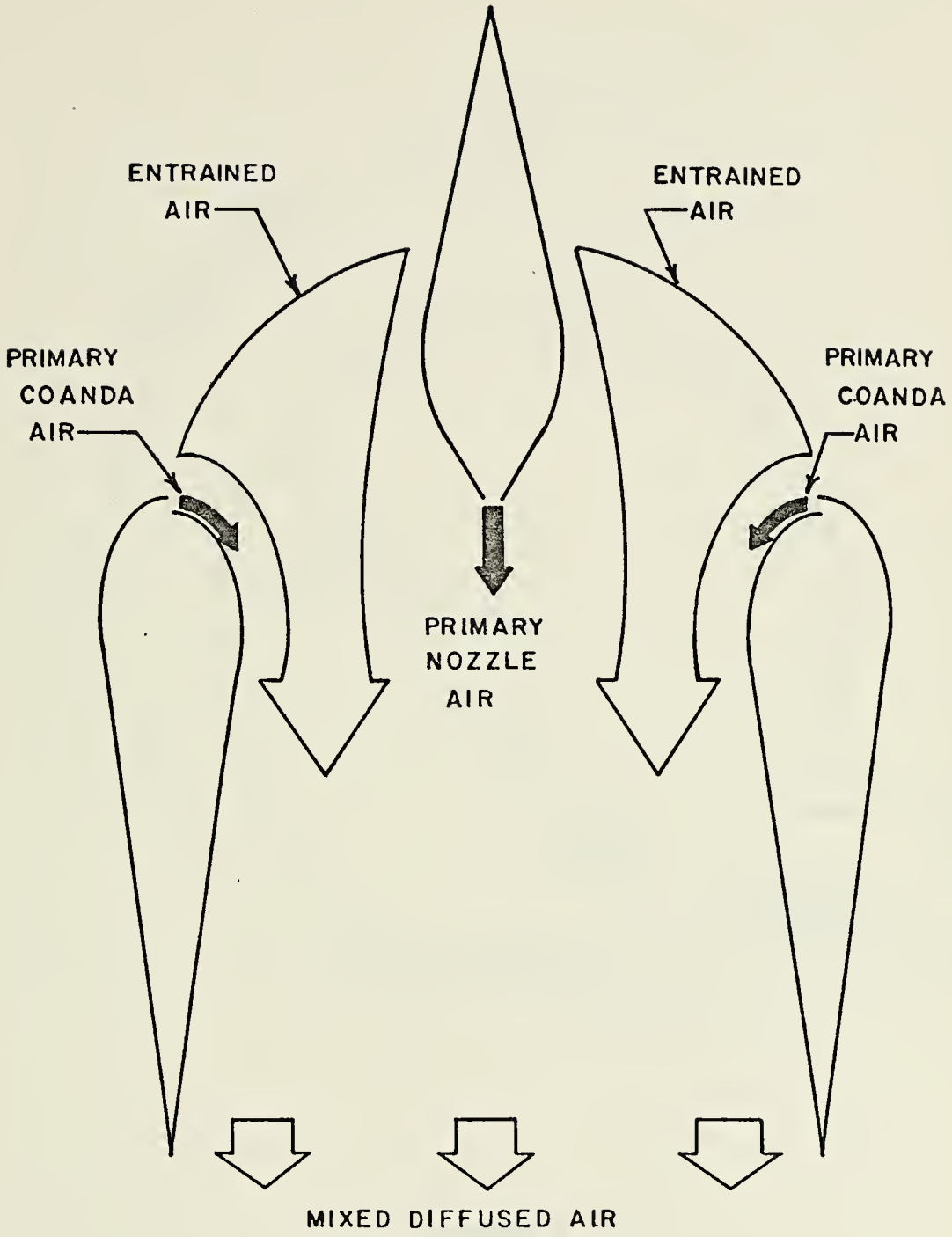

FIGURE 2. COANDA BLOWING

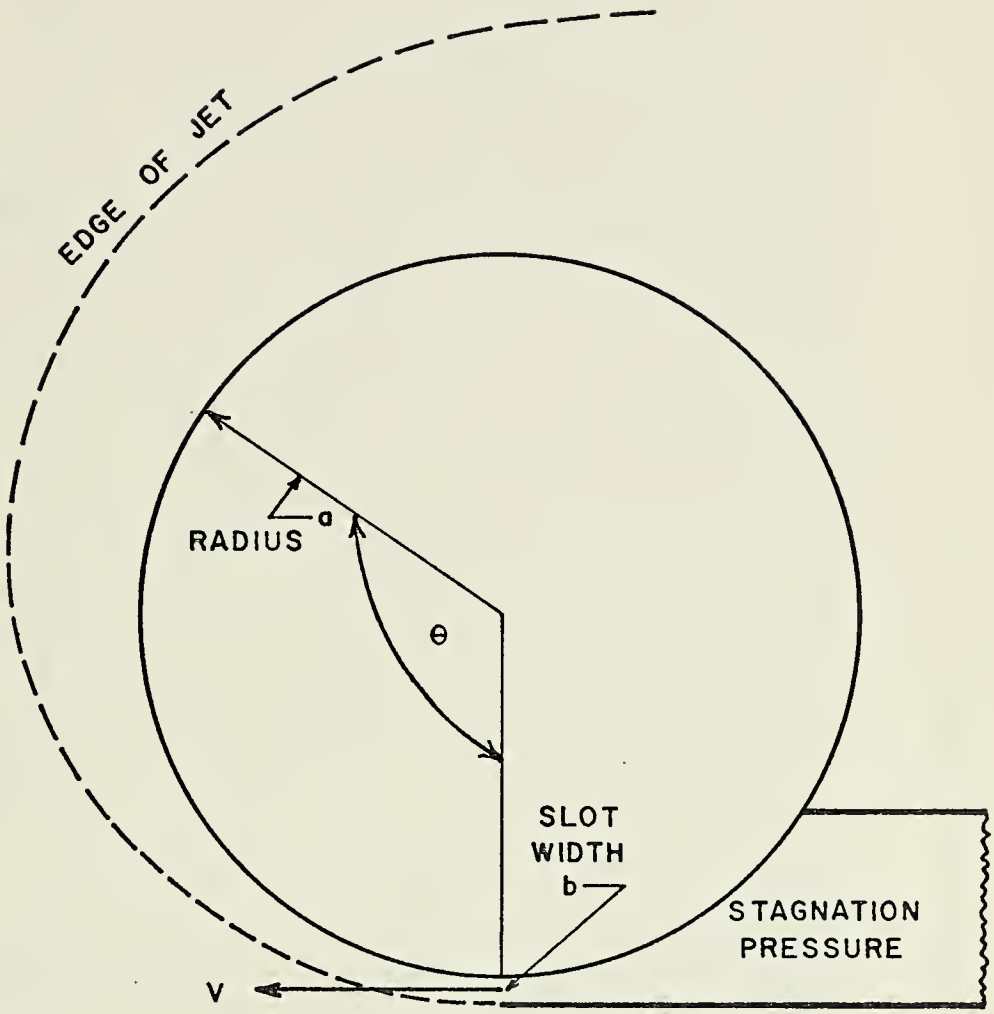

FIGURE 3.

FLOW OF A TWO-DIMENSIONAL JET AROUND A CIRCULAR CYLINDER

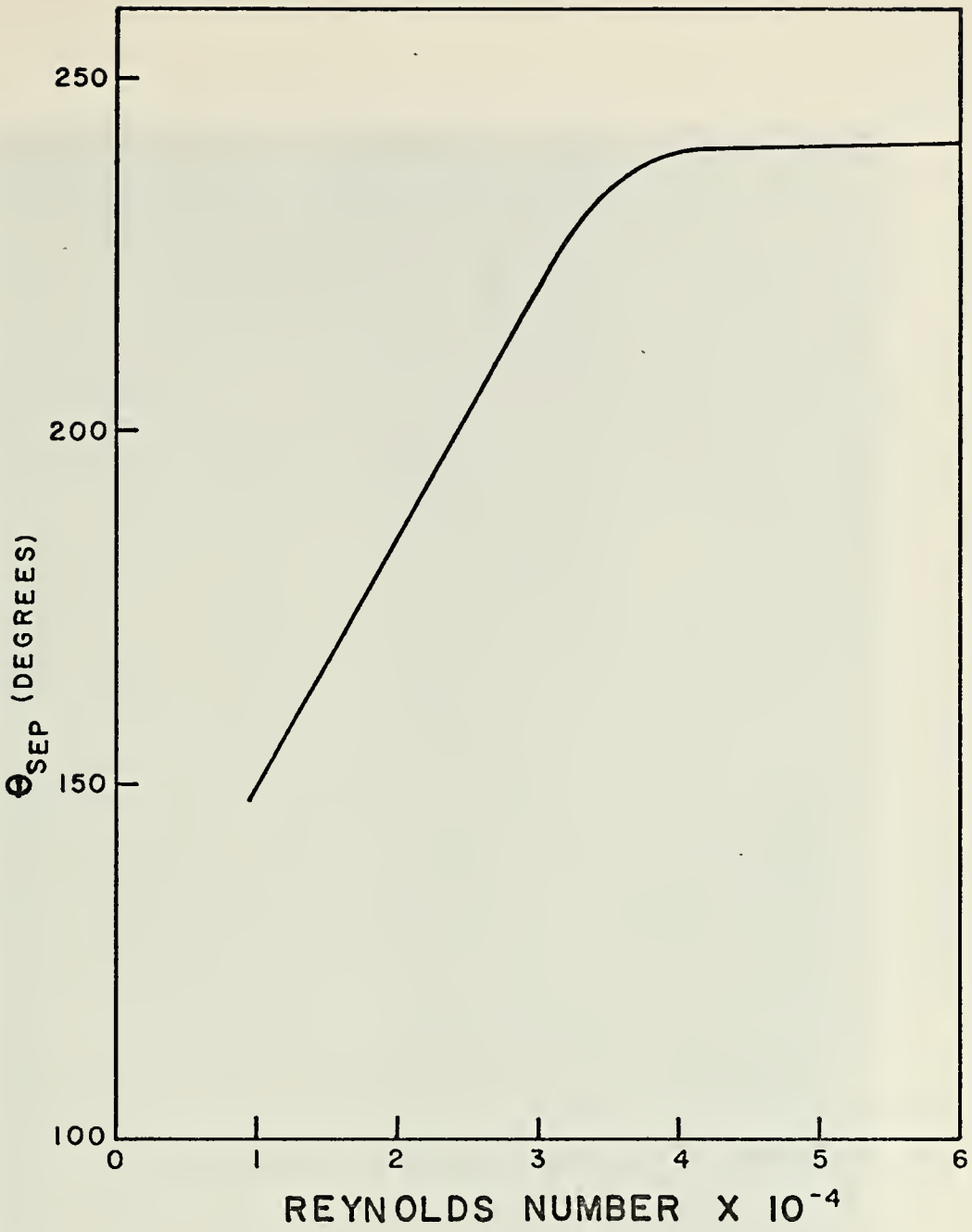

FIGURE 4.
$\theta_{SEPARATION}$ VS. REYNOLDS NUMBER

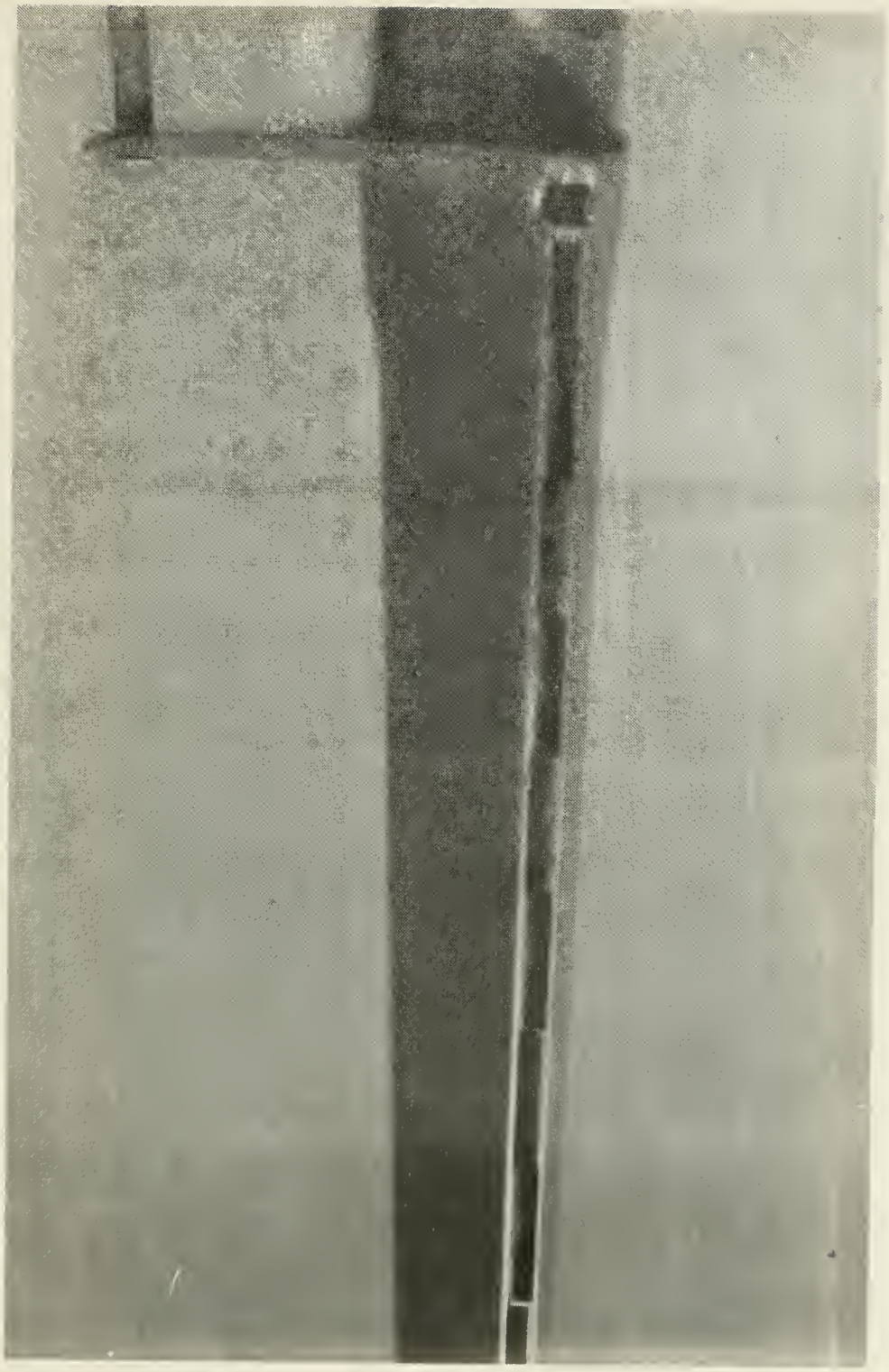

FIGURE 5. HYPERMIXING NOZZLE

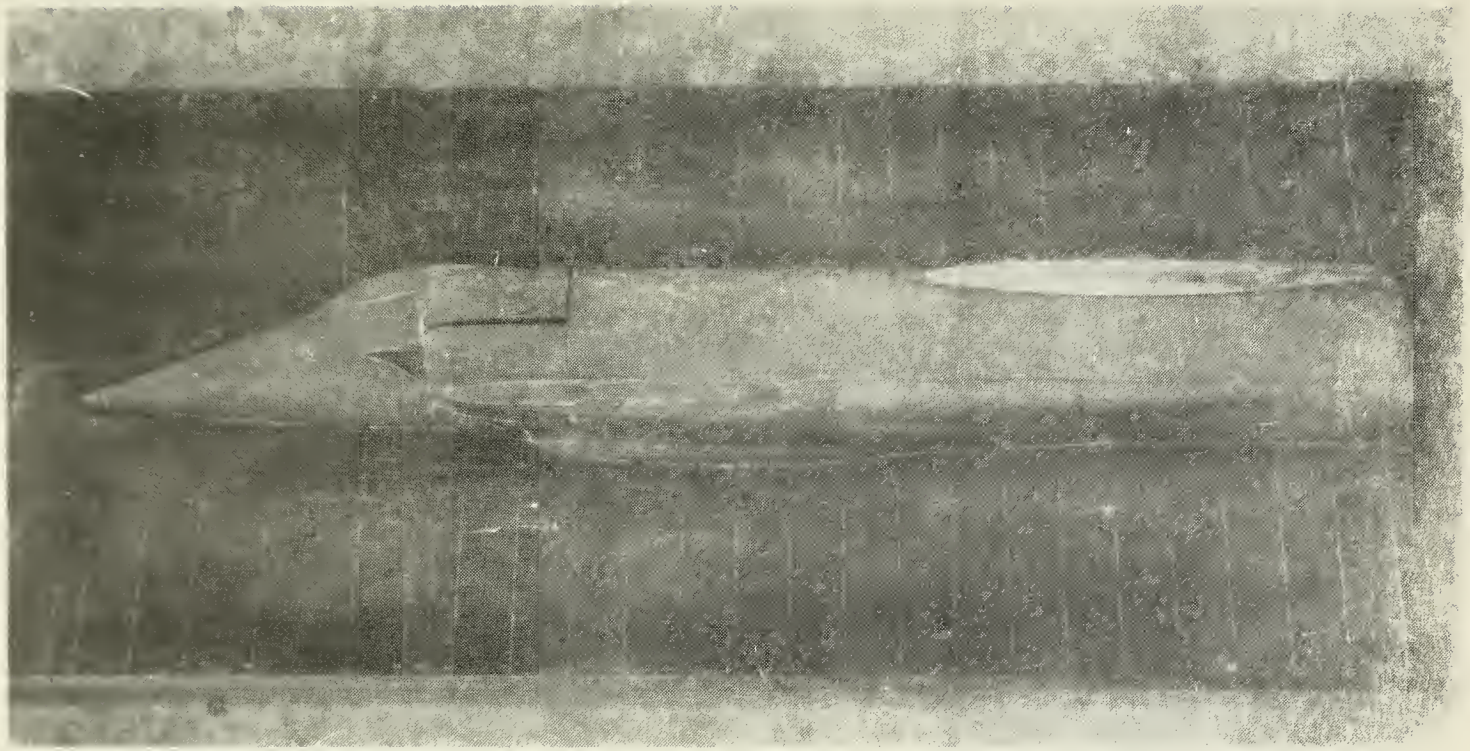

FIGURE 6. CLAY MALE MOLD FOR MODEL FUSELAGE

FIGURE 7. MODEL FUSELAGE WITH WING AND CANARD ATTACHED

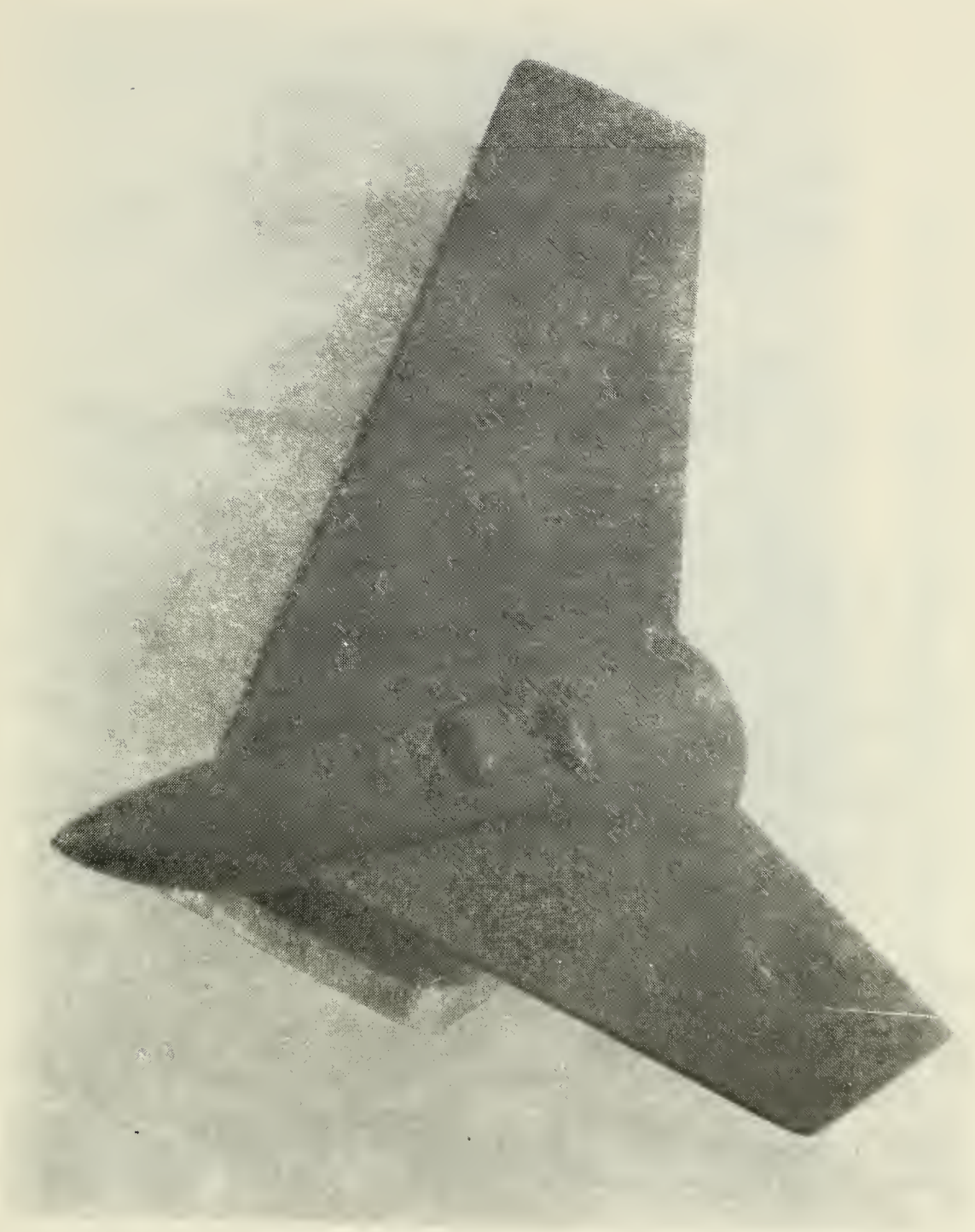

FIGURE 8. VERTICAL TAIL ASSEMBLY

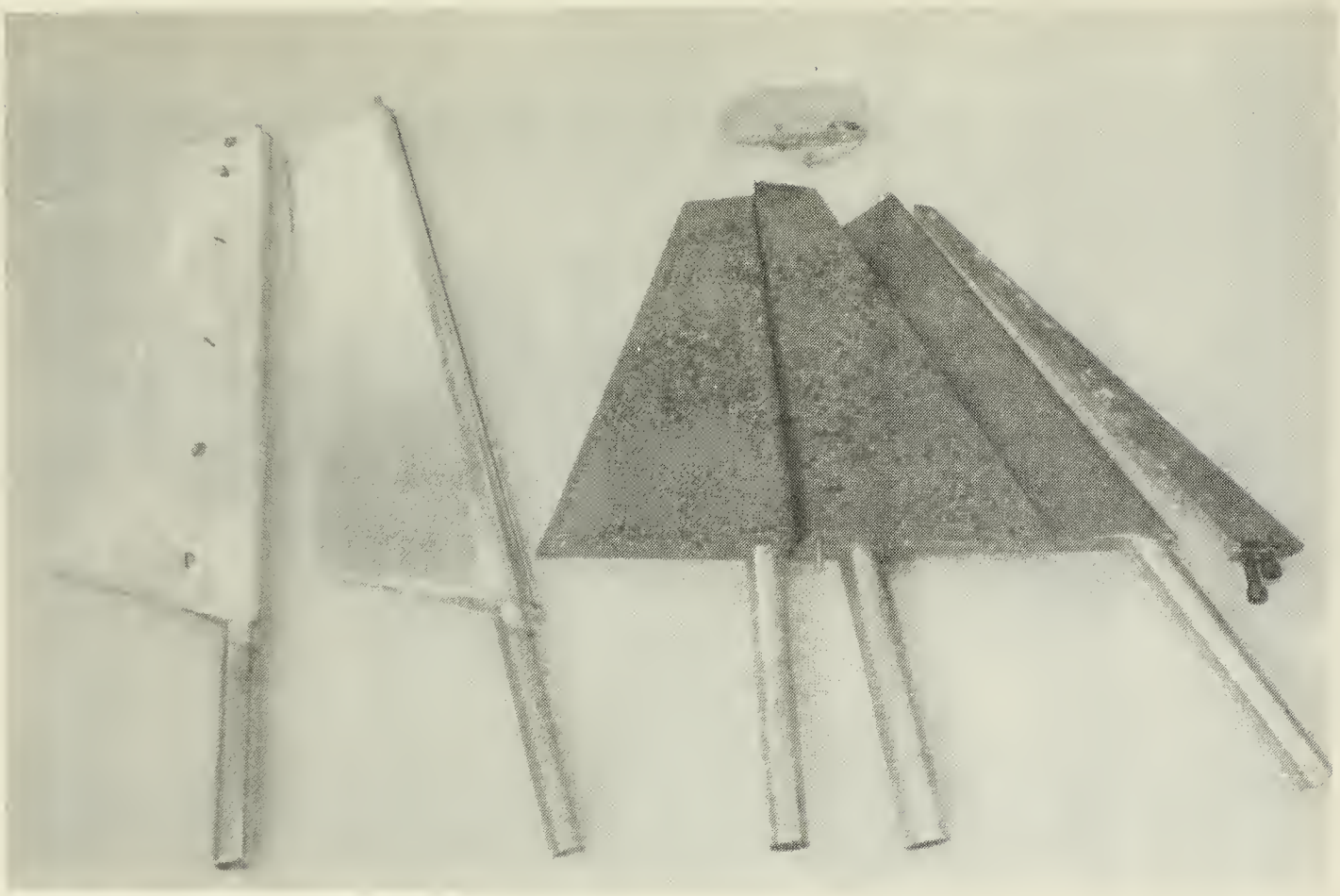

FIGURE 9. EJECTOR COMPONENT DETAILS (TOP VIEW)

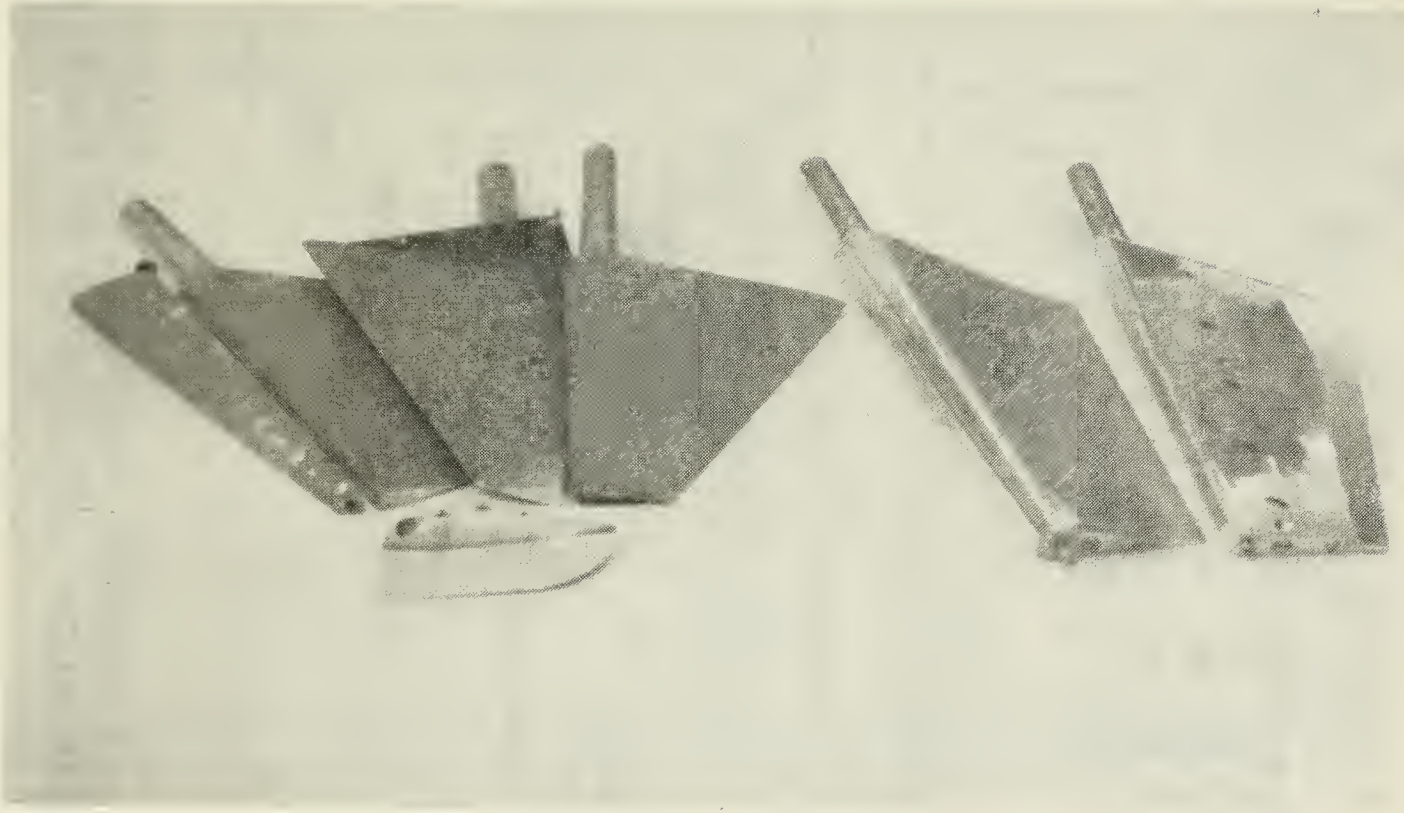

FIGURE 10. EJECTOR COMPONENT DETAILS (SIDE VIEW)

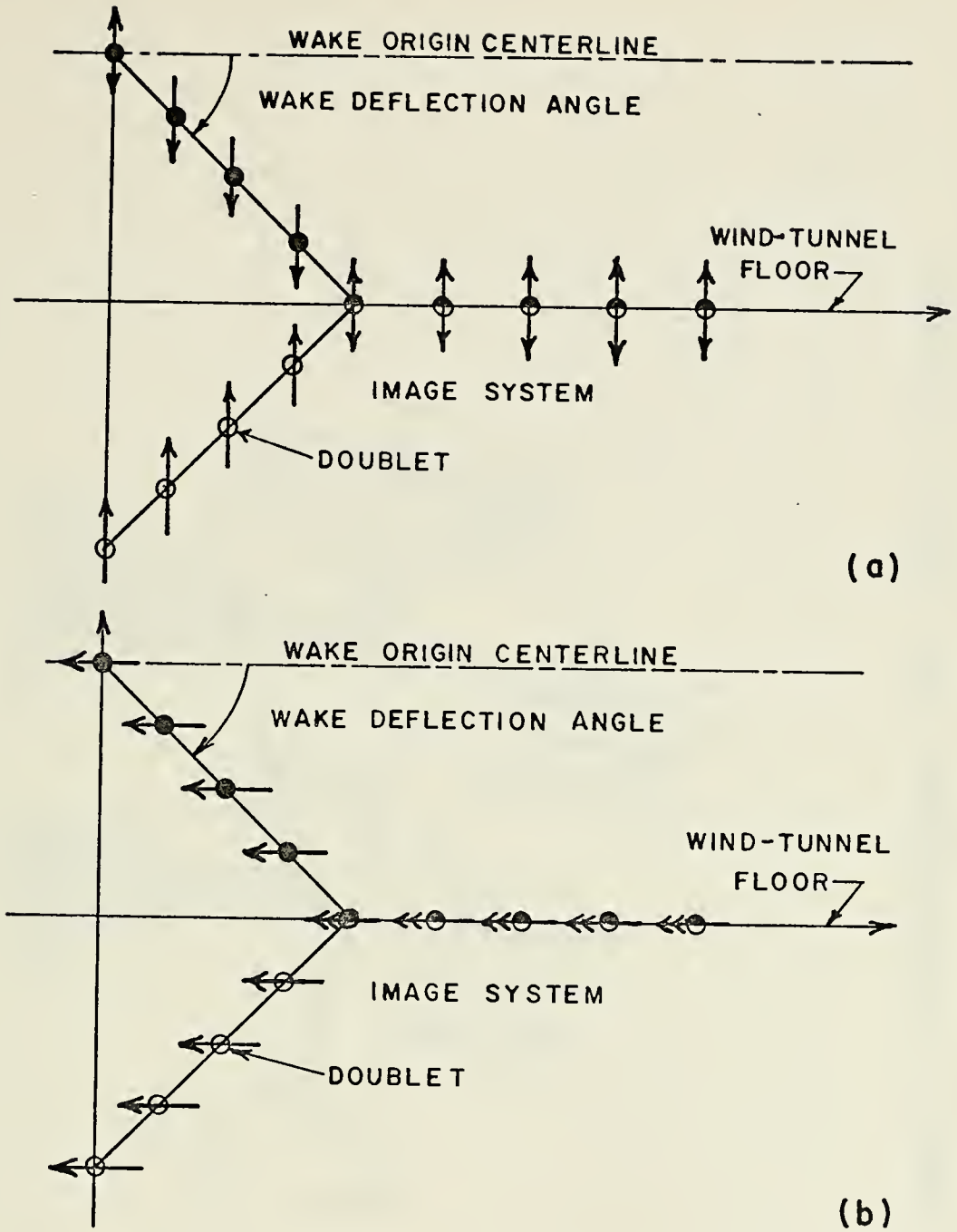

(a) WAKE OF VERTICAL DOUBLETS
(b) WAKE OF HORIZONTAL DOUBLETS

FIGURE 11.

WAKE AND IMAGE SYSTEM

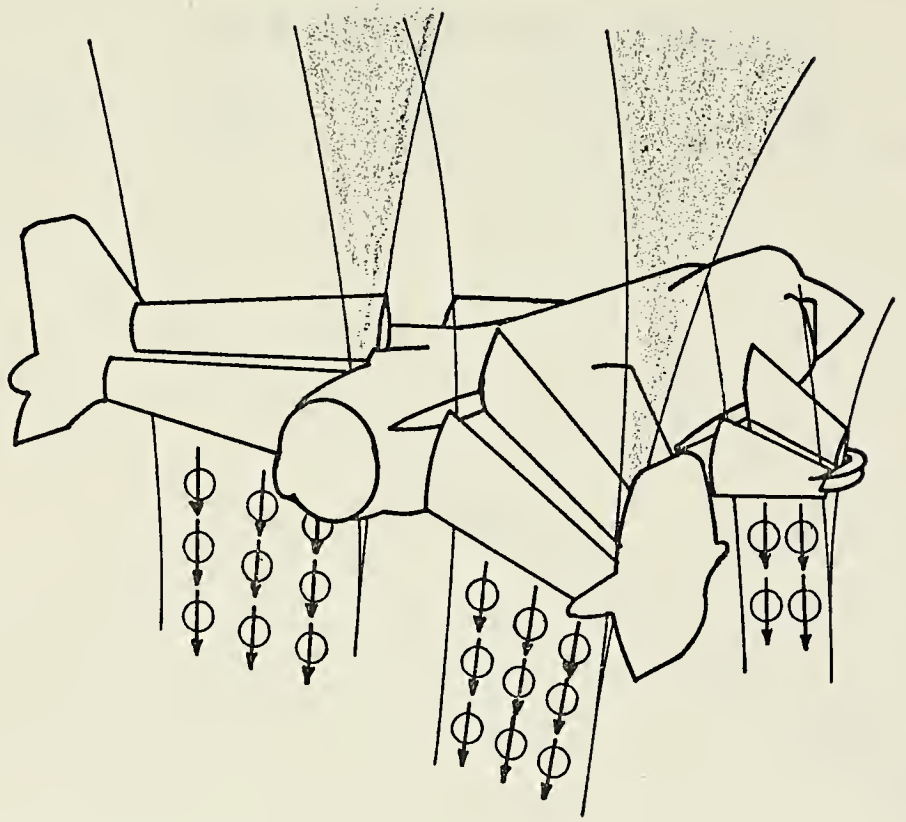

FIGURE 12. FLOW MODELING WITH DOUBLET SHEETS

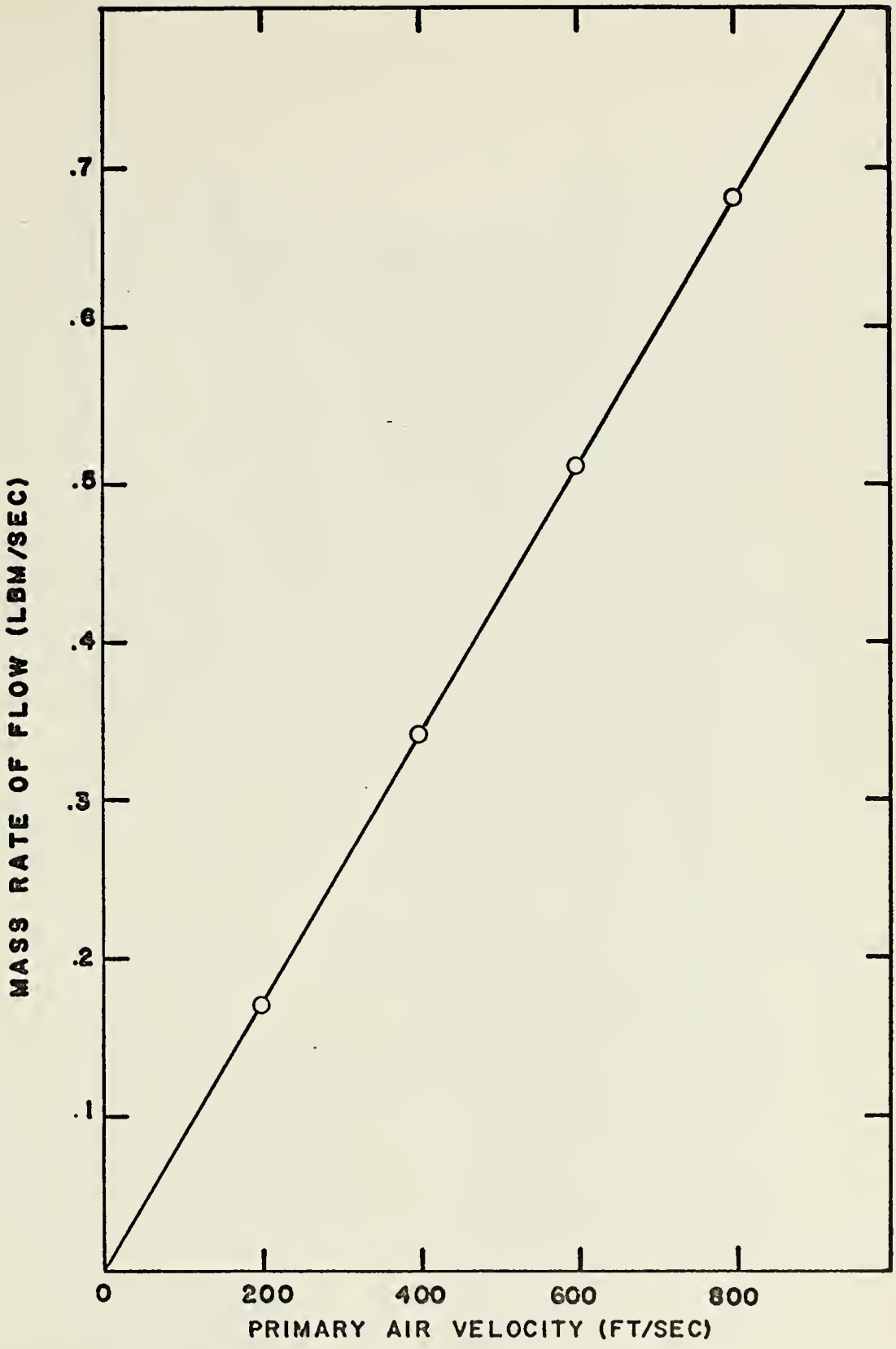

FIGURE 13. MASS RATE OF FLOW VS. PRIMARY AIR VELOCITY

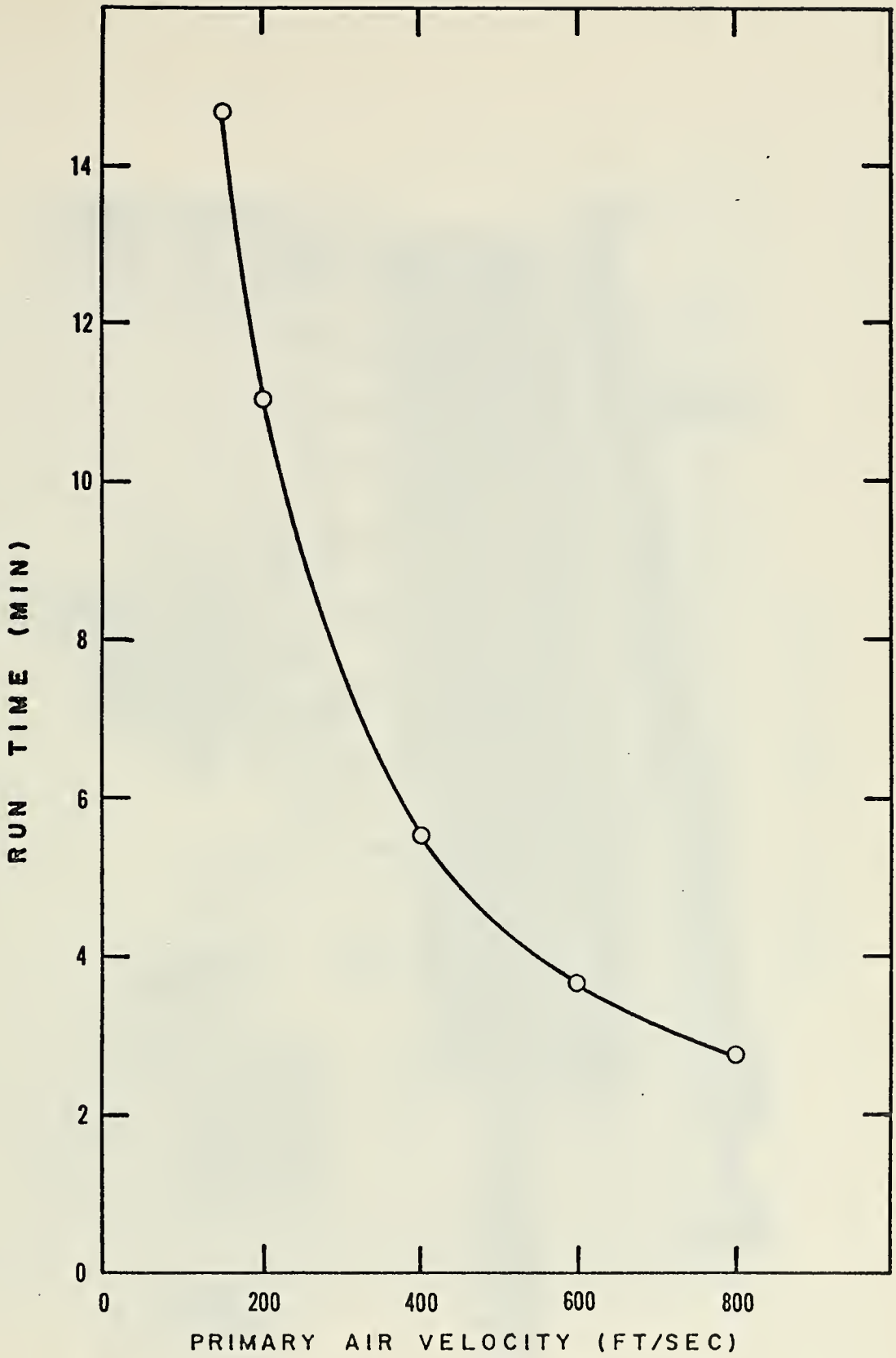

FIGURE 14. RUN TIME VS. PRIMARY AIR VELOCITY

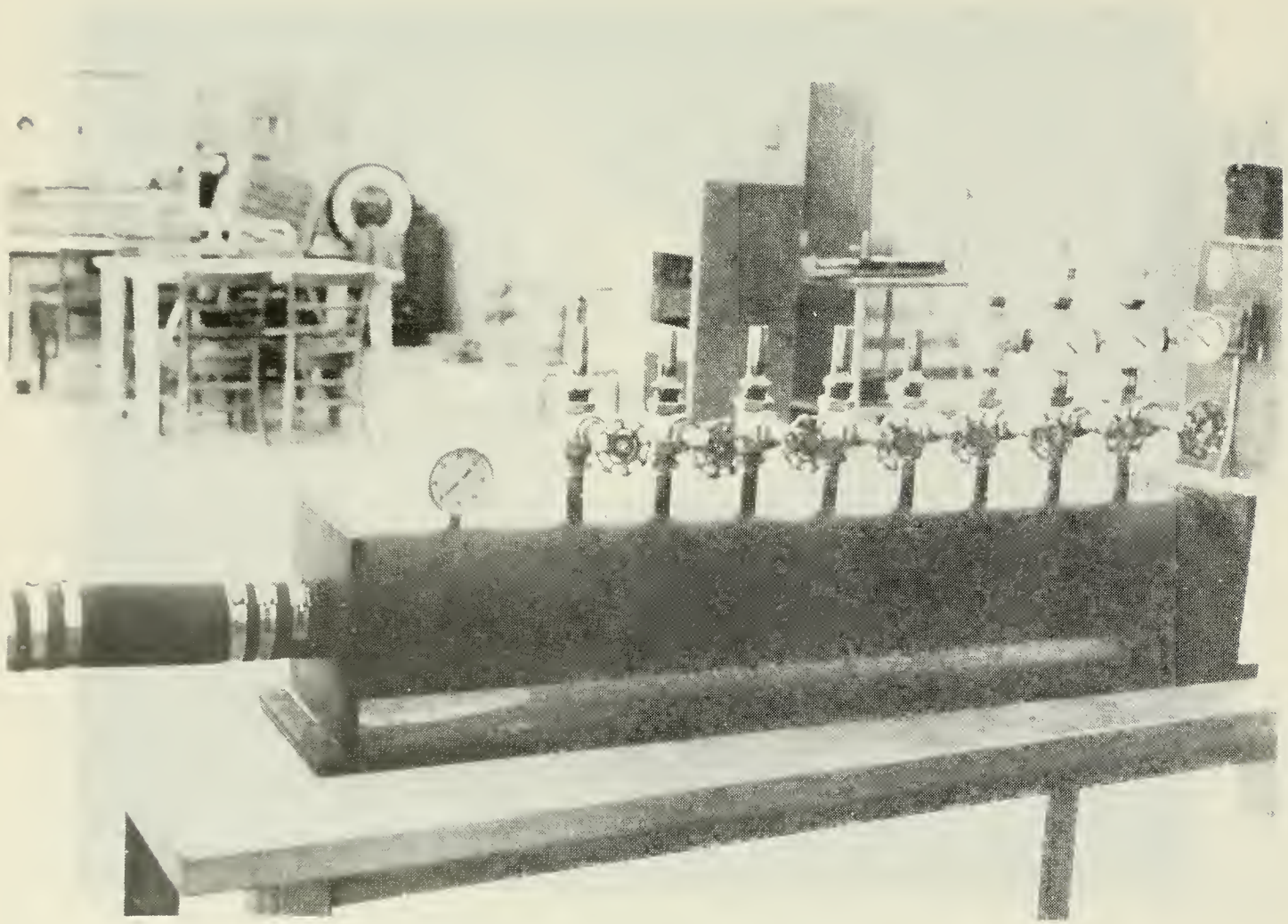

FIGURE 15. SYSTEM PLENUM

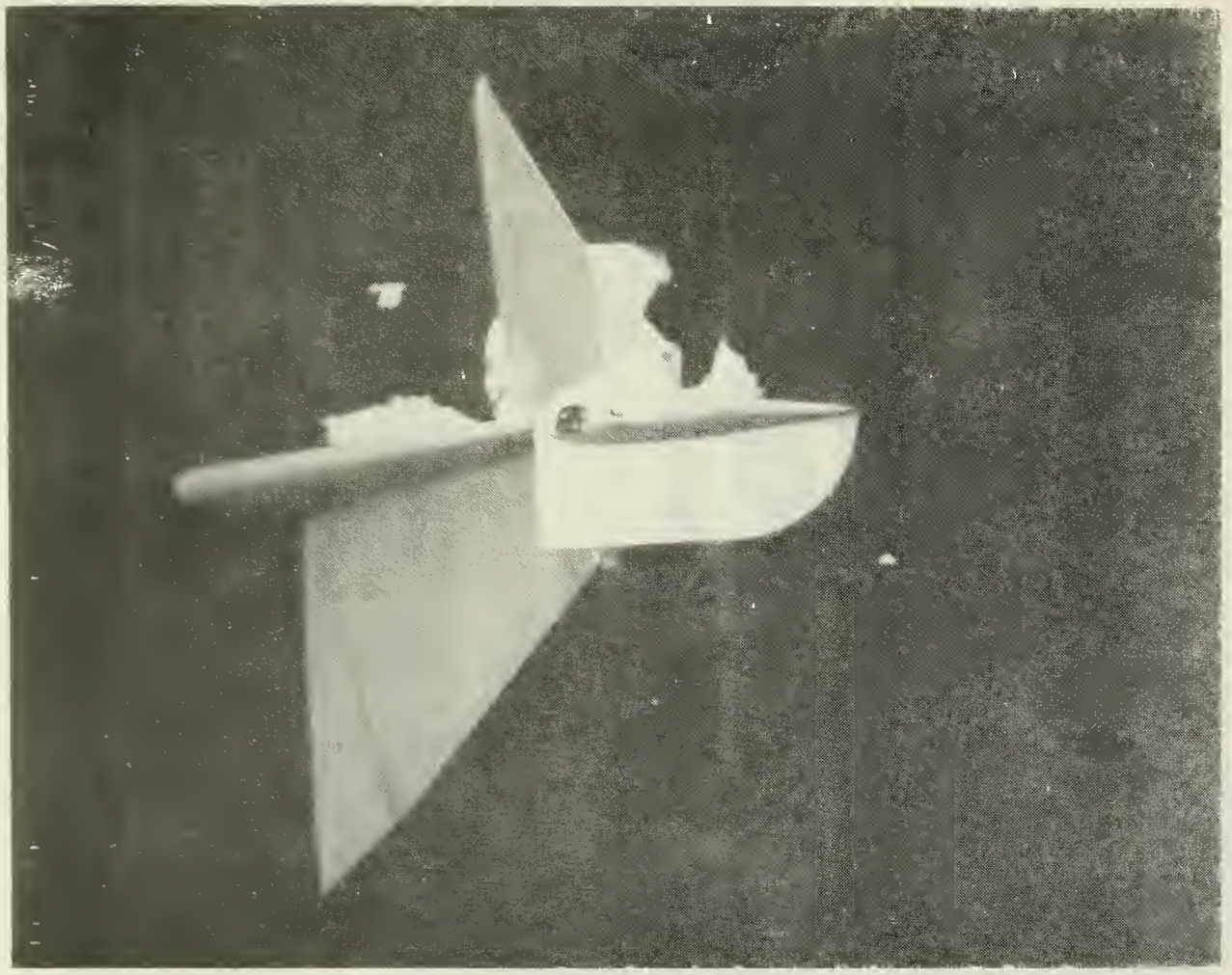

FIGURE 16. CANARD DIFFUSER

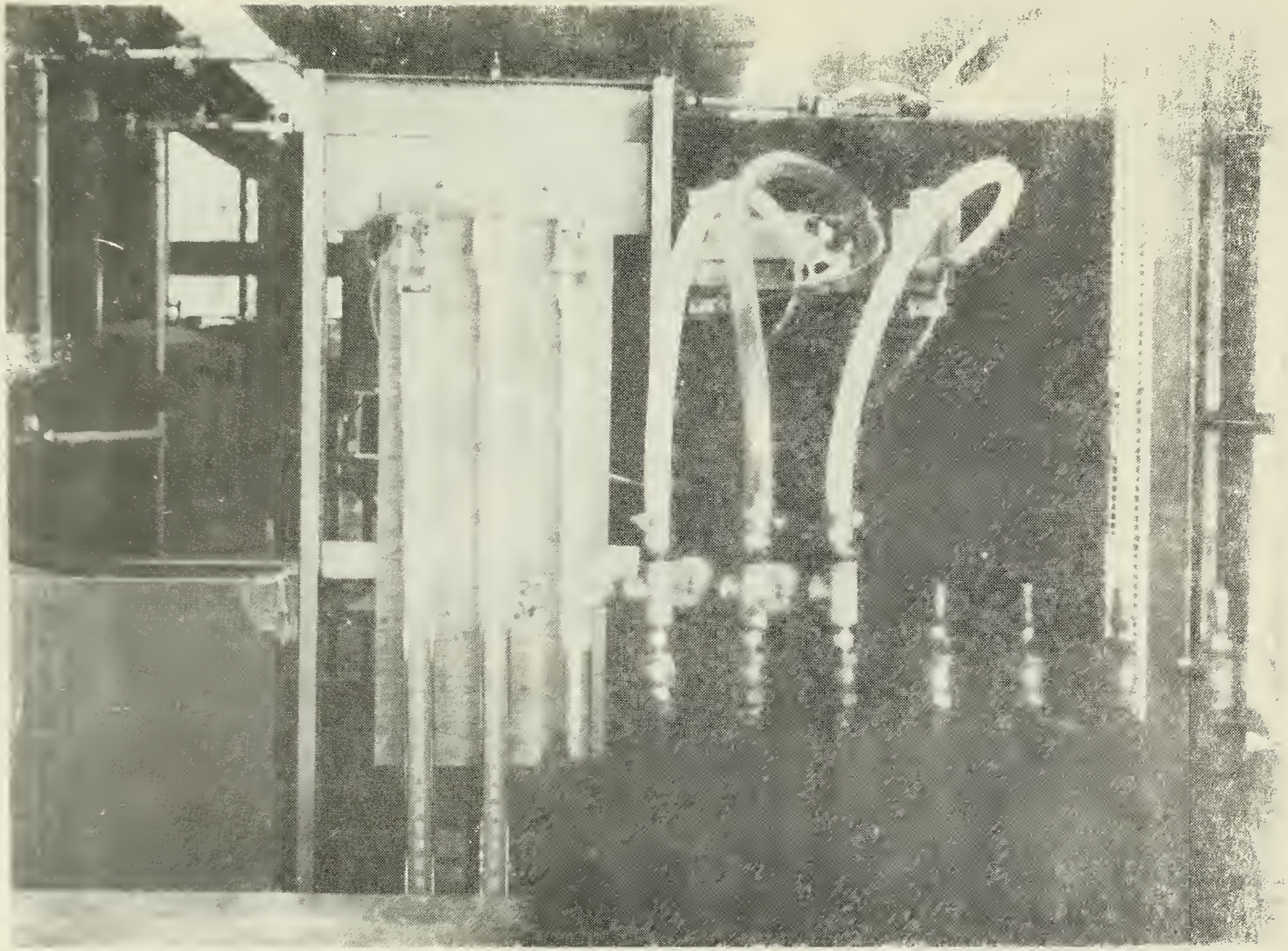

FIGURE 17. CANARD TEST APPARATUS (BACK VIEW)

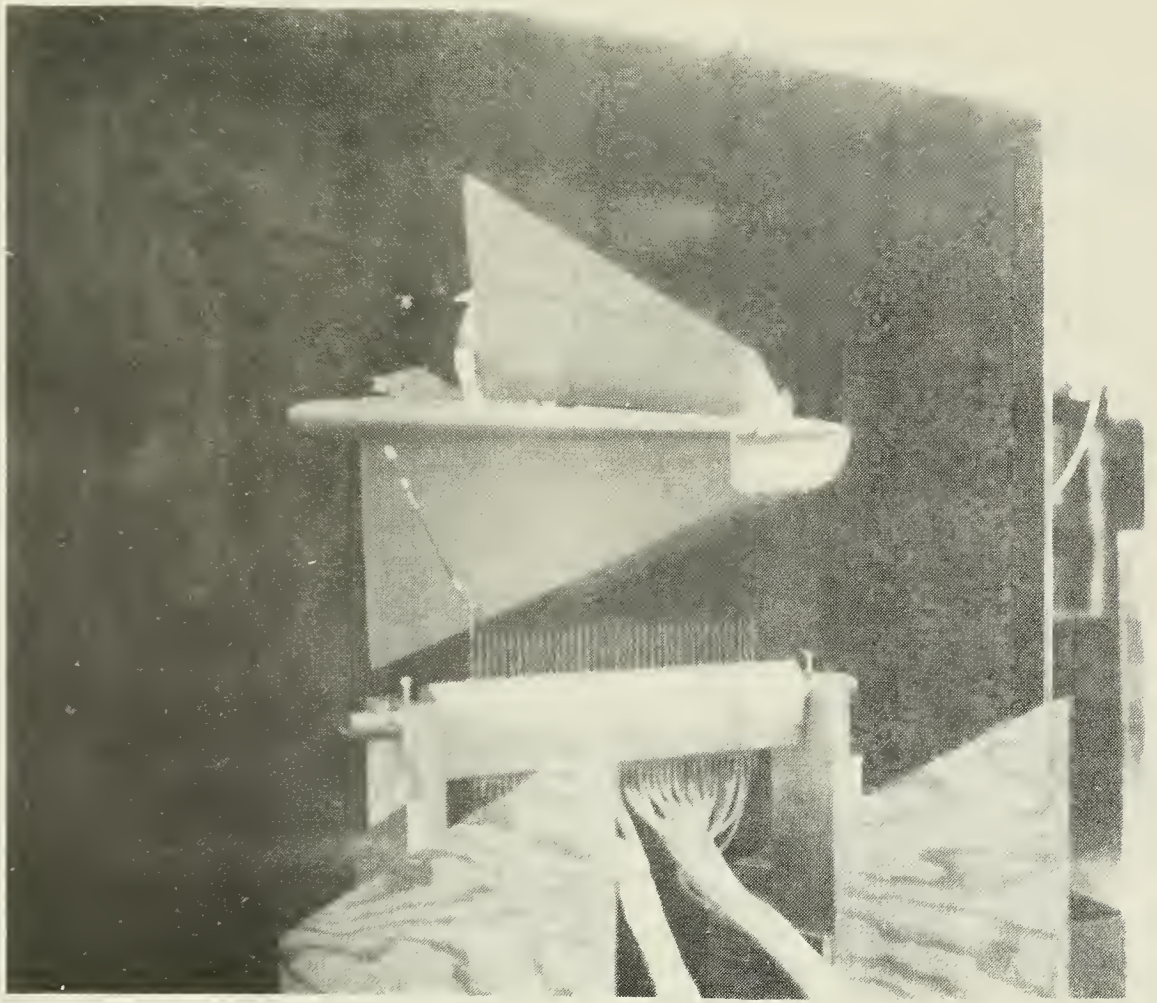

FIGURE 18. CANARD TEST APPARATUS (FRONT VIEW)

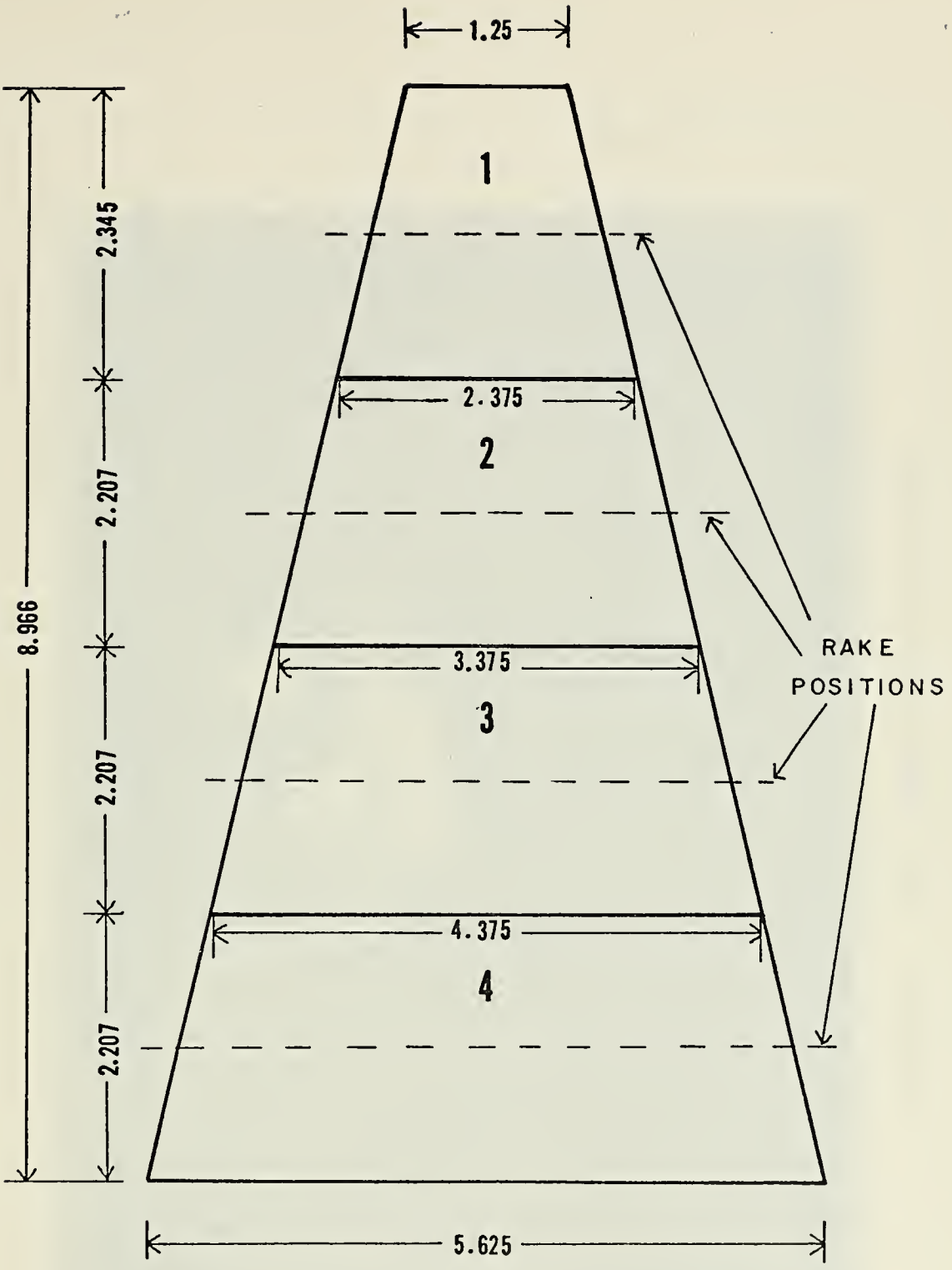

FIGURE 19. AREA DIVISION FOR PRESSURE SURVEY

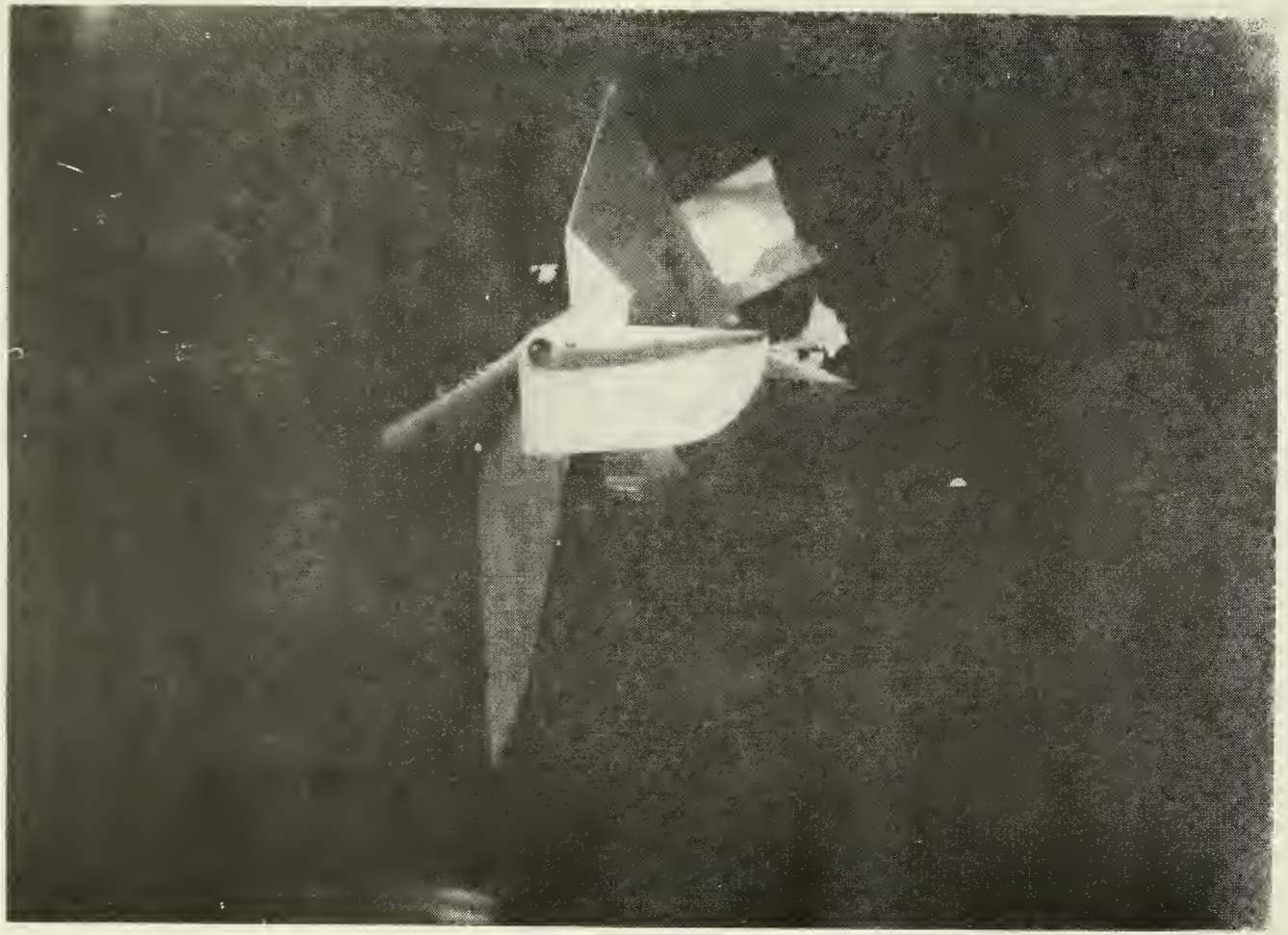

FIGURE 20. FLOW VISUALIZATION WITH TUFTS

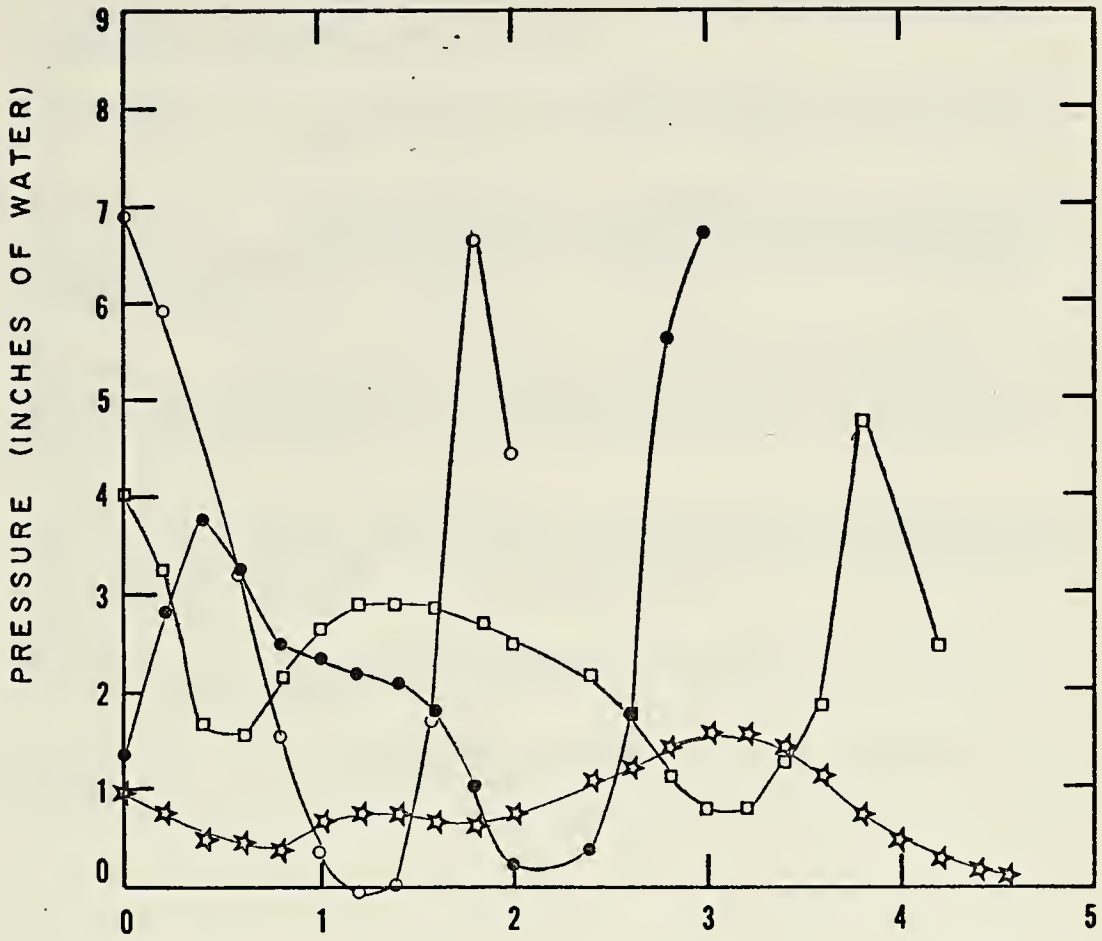

FIGURE 21. PRESSURE SURVEYS

LIST OF REFERENCES

1. Heyson, H. H., Linearized Theory of Wind-Tunnel Jet-Boundary Corrections and Ground Effect for VTOL-STOL Aircraft, NASA TR R-124, 1962.

2. Karamcheti, K., Principles of Ideal-Fluid Aerodynamics, John Wiley and Sons, Inc., New York, 1966.

3. Newman, B. G., The Deflexion of Plane Jets By Adjacent Boundaries — Coanda Effect. Boundary Layer and Flow Control, Volume I, Edited by Lachman, G. V., Pergamon Press, 1961.

4. Quinn, B., Recent Developments in Large Area Ratio Thrust Augmentors, AIAA paper number 72-1174, American Institute of Aeronautics and Astronautics, New York, 1972.

5. Quinn, B., Thrust Augmenting Ejectors for V/STOL Aircraft, Proceedings of the Air Force Science and Engineering Symposium, Volume I, 17 August 1972.

6. Stratton, J. A., Electromagnetic Theory, p. 191-193, McGraw Hill, 1941.

7. Streeter, V. L., Fluid Mechanics, p. 219, McGraw-Hill, 1971.

INITIAL DISTRIBUTION LIST

		No. Copies
1.	Defense Documentation Center Cameron Station Alexandria, Virginia 22314	2
2.	Library, Code 0212 Naval Postgraduate School Monterey, California 93940	2
3.	Department Chairman, Code 57 Department of Aeronautics Naval Postgraduate School Monterey, California 93940	2
4.	Professor A. E. Fuhs, Code 57Fu Department of Aeronautics Naval Postgraduate School Monterey, California 93940	4
5.	Lcdr. J. E. Killian, USN VA-174 Cecil Field Jacksonville, Florida 32212	3
6.	Lt. A. T. Doryland, USN HS-10 NAS Imperial Beach Imperial Beach, California 92032	2
7.	Mr. R. F. Siewert, Code 320D Naval Air Systems Command Washington, D.C. 20360	2
8.	Captain R. L. Von Gerichten, USN VTOL Program Officer Naval Air Systems Command Washington, D.C. 20360	1
9.	Dr. Brian Quinn A.R.L. Wright-Patterson AFB Dayton, Ohio 45433	1
10.	Mr. V. R. Hancock XFV-12A Program Manager Columbus Aircraft Division North American Rockwell 4300 East Fifth Avenue Columbus, Ohio 43216	1

11. Captain A. A. Schaufelberger, USN — 1
Code PDMA-1
Naval Air Systems Command
Washington, D.C. 20360

12. Mr. John Tankersley — 1
Columbus Aircraft Division
North American Rockwell
4300 East Fifth Avenue
Columbus, Ohio 43216

13. Mr. Robert M. Williams — 1
Aviation and Surface Effects Department
Naval Ship Research and Development Center
Bethesda, Maryland 20034

SECURITY CLASSIFICATION OF THIS PAGE (When Data Entered)

REPORT DOCUMENTATION PAGE		READ INSTRUCTIONS BEFORE COMPLETING FORM
1. REPORT NUMBER	2. GOVT ACCESSION NO.	3. RECIPIENT'S CATALOG NUMBER
4. TITLE (and Subtitle) Construction of One-Tenth Scale Model of the XFV-12A and Canard Performance Test		5. TYPE OF REPORT & PERIOD COVERED Master's Thesis; March 1974 6. PERFORMING ORG. REPORT NUMBER
7. AUTHOR(s) James Edward Killian Adrian Tracy Doryland		8. CONTRACT OR GRANT NUMBER(s)
9. PERFORMING ORGANIZATION NAME AND ADDRESS Naval Postgraduate School Monterey, California 93940		10. PROGRAM ELEMENT, PROJECT, TASK AREA & WORK UNIT NUMBERS
11. CONTROLLING OFFICE NAME AND ADDRESS Naval Postgraduate School Monterey, California 93940		12. REPORT DATE March 1974 13. NUMBER OF PAGES 62
14. MONITORING AGENCY NAME & ADDRESS(if different from Controlling Office) Naval Postgraduate School Monterey, California 93940		15. SECURITY CLASS. (of this report) Unclassified 15a. DECLASSIFICATION/DOWNGRADING SCHEDULE

16. DISTRIBUTION STATEMENT (of this Report)

Approved for public release; distribution unlimited.

17. DISTRIBUTION STATEMENT (of the abstract entered in Block 20, if different from Report)

18. SUPPLEMENTARY NOTES

19. KEY WORDS (Continue on reverse side if necessary and identify by block number)

20. ABSTRACT (Continue on reverse side if necessary and identify by block number)

The XFV-12A is a high-performance, VTOL, fighter/attack aircraft which incorporates ejectors in the wings and canards for thrust augmentation. During transition from VTOL to normal flight, the interaction between downflow of the lifting jets and relative flow from forward flight generates vortices distinct from airfoil circulation. These vortices are associated with the bending of the lifting jets resulting in

DD FORM 1 JAN 73 1473 EDITION OF 1 NOV 65 IS OBSOLETE
S/N 0102-014-6601 |
(Page 1)

SECURITY CLASSIFICATION OF THIS PAGE (When Data Entered)

(20. ABSTRACT continued)

induced velocities at the aircraft; the magnitude and influence of the vortices are unknown. The object of this thesis was to prepare a suitable one-tenth scale semi-span model of the XFV-12A for smoke tunnel flow visualization study to explore vortex development. Performance testing was conducted on the canard augmentor, which resulted in a gross augmentation ratio of 1.34 and mass flow ratio of 6.84.